計畫編號：NHRI-EX93-9324NC

國家衛生研究院整合性醫藥衛生科技研究計畫

探討急性酒精暴露對老鼠巨噬細胞的影響

計畫名稱

九十三年度成果報告

執 行 機 構：中山醫學大學

計 畫 主 持 人：吳文俊

本年度執行期間： 93 年 1 月 1 日 至 93 年 12 月 31 日

計畫編號：NHRI-EX93-9324NC

國家衛生研究院整合性醫藥衛生科技研究計畫

探討急性酒精暴露對老鼠巨噬細胞的影響

計畫名稱

九十三年度成果報告

執 行 機 構：中山醫學大學

計 畫 主 持 人：吳文俊

本年度執行期間： 93 年 1 月 1 日 至 93 年 12 月 31 日

計畫名稱：探討急性酒精暴露對老鼠巨噬細胞的影響

計畫編號：NHRI-EX93-9324NC

執行機構：中山醫學大學

計畫主持人：吳文俊

研究人員：許華偉、徐志欣、鍾艾玲

關鍵字：酒精，巨噬細胞，免疫抑制，神經內分泌物質

壹、 九十三年度計畫研究成果摘要

根據研究顯示慢性酒精中毒者和有酒癮者罹患傳染病的機會比一般非酗酒者還要高，原因在於這些酗酒者的免疫功能已被抑制，故較不能抵抗外來的疾病。另有證據指出在一夕之間飲酒狂歡的人數並不少於慢性酒精中毒者，然而有關免疫功能在這些急性酒精中毒者的情形所知仍有限。本人以前的研究顯示餵與單一劑量的酒精在老鼠體內可以抑制自然殺手細胞(natural killer cells)的功能。巨噬細胞 (macrophages) 在疾病的防禦上扮演一重要的角色，其對緊迫反應的敏感性不得而知。故本計劃將探討急性酒精暴露對一般的和活化的老鼠巨噬細胞數目及其免疫功能的影響。巨噬細胞可被多種刺激物所活化，這些被活化後的巨噬細胞比一般的巨噬細胞更能有效的殺死微生物或腫瘤細胞，因此被活化後的巨噬細胞比一般的巨噬細胞扮演更重要的免疫防禦功能。在本計劃下巨噬細胞將被一種物質叫 thioglycollate 所活化，這些被 thioglycollate 所活化後的巨噬細胞功能和被微生物所活化後的情形十分類似。本計劃將探討急性酒精暴露如何影響巨噬細胞，藉由誘發何種內分泌物質進而導致巨噬細胞數目及其免疫功能的下降。本篇研究以 B6C3F1 母鼠為實驗動物，32 %（6.0 g/kg）的酒精劑量為實驗劑量，探討在急性酒精暴露下，對腹腔內巨噬細胞的細胞數目及其免疫功能，包括吞噬作用、釋放過氧化氫、一氧化氮及腫瘤壞死因子能力和毒殺腫瘤細胞能力的影響。研究結果發現酒精會減少腹腔巨噬細胞的細胞

數目及抑制上述所列之免疫功能。另外加入 thioglycollate 模擬生物體受到細菌感染時的情形，也發現酒精會降低腹腔巨噬細胞數目及其免疫功能。我們也使用 RU486(糖皮質素受器的拮抗劑)探討糖皮質素(glucocorticoids)對急性酒精降低腹腔巨噬細胞的細胞數目及抑制免疫功能所扮演的角色，結果顯示酒精誘導生成的糖皮質素的確會在這方面對其造成影響。

Studies of human subjects have shown that chronic ethanol ingestion is associated with abnormalities of humoral and cellular immunity. These abnormalities may contribute to the increased incidence of infectious diseases and even cancer in alcoholics. Chronic ethanol administration also damages a broad spectrum of immune functions in experimental animals. Binge drinking of ethanol is probably more common than chronic heavy drinking, and this has become a serious problem among young persons. While chronic effects of ethanol on the immune system have been studied extensively, less information is available regarding immunosuppressive effects of acute ethanol exposure. Our previous studies have shown that a single dose of ethanol could suppress natural killer cell activity in a mouse model. Macrophages play an important role in host resistance to microbes and tumor cells. The sensitivity of various lymphocytes to ethanol may be different. Therefore, the present project will evaluate the effects of ethanol on the murine peritoneal macrophages after a single dose of ethanol by gavage. Also, this project will evaluate the role of neuroendocrine mediators involved in the immunosupression of murine peritoneal macrophages. In this study, we investigated the effects of ethanol on the murine peritoneal macrophage cellularity and immune functions after a single dose of ethanol by gavage. The immune functions of macrophages including phagocytosis, hydrogen peroxide (H_2O_2) production, nitric oxide (NO), TNF-α release and tumoricidal activity. The results showed that ethanol decreased macrophage number and inhibited the above-mentioned immune functions in a time-dependent manner. In addition, we found the similar phenomena of ethanol on thioglycollate-elicited macrophages. We used RU486 (glucocorticoid receptor antagonist) to explore the role of ethanol in

decreasing macrophage number and inhibiting macrophage functions. The result indicated that ethanol induced the production of glucocorticoids that were involved in this process.

貳、九十三年度計畫著作一覽表

註：群體計畫(PPG)者，不論是否提出各子計畫資料，都必須提出總計畫整合之資料

若為群體計畫，請勾選本表屬於：□子計畫； 或 □總計畫(請自行整合)

1.列出貴計畫於本年度中之<u>所有計畫產出</u>於下表，包含已發表或已被接受發表之文獻、已取得或被接受之專利、擬投稿之手稿（manuscript）以及專著等

2.「計畫產出名稱」欄位：請依「臺灣醫誌」參考文獻方式撰寫

3.「產出型式」欄位：填寫該產出為國內期刊、國外期刊、專利、手稿或專著等

4.「SCI/SSCI」欄位：Social/Science Citation Index，若發表之期刊為 SCI/SSCI 所包含者，請在欄位上填寫該期刊當年度之 impact factor

5.「致謝與否」欄位：請註明該成果產出之致謝單位。若該成果產出有註明衛生署資助字樣者，請以 DOH 註明；若該成果產出有註明國家衛生研究院委託資助字樣者，請以 NHRI 註明；若該成果產出有註明衛生署及國家衛生研究院資助字樣者，請合併以 DOH&NHRI 註明；若該成果產出有註明非上述機構資助字樣者，請以機構全銜註明，舉例如下：

序號	計畫產出名稱	產出型式	SCI/SSCI	致謝與否
1.	Wu, M.-F., Wu, W.-J. Chang, G.-C., Chen, C.-Y., Hu, S.-W., Tsai, W.-T., Lee, H., and Lin, P. Increased expression of cytochrome P4501B1 in peripheral leukocytes from lung cancer patients. Toxicol. Lett. 2004;150: 211-219.	國外期刊	2.224	NSC
2.	Hsu, T.-C, Wu, W.-J. Chen, M.-C., and Tsay GJ. Human parvovirus B19 non-structural protein (NS1) induces apoptosis through mitochondria cell death pathway in COS-7 cells. Scand. J. Infect. Dis. 2004;36: 570-7.	國外期刊	1.117	NSC
3.				
4.				
5.				
6.				
7.				
8.				
9.				

*本表如不敷使用，請自行影印。

參、九十三年度計畫重要研究成果產出統計表

註：群體計畫(PPG)者，不論是否提出各子計畫資料，都必須提出總計畫整合之資料
若為群體計畫，請勾選本表屬於: □子計畫； 或 □總計畫(請自行整合)

(係指執行九十三年度計畫之所有研究產出成果)

<table>
<tr><td colspan="3">科 技 論 文 篇 數</td><td colspan="3">技 術 移 轉</td></tr>
<tr><td></td><td>國 內</td><td>國 外</td><td>類 型</td><td>經 費</td><td>項 數</td></tr>
<tr><td>期 刊
論 文</td><td>篇</td><td>2 篇</td><td>技 術
輸 入</td><td>千元</td><td>項</td></tr>
<tr><td>研討會
論 文</td><td>2 篇</td><td>篇</td><td>技 術
輸 出</td><td>千元</td><td>項</td></tr>
<tr><td>專 著</td><td>篇</td><td>篇</td><td>技 術
擴 散</td><td>千元</td><td>項</td></tr>
<tr><td colspan="2">技術報告</td><td colspan="2">技術創新</td><td colspan="2">著作權</td><td>專利權</td></tr>
<tr><td colspan="2" rowspan="2">篇</td><td colspan="2" rowspan="2">項</td><td colspan="2">(核准) 項</td><td>(核准) 項</td></tr>
<tr><td colspan="2">(申請中) 項</td><td>(申請中) 項</td></tr>
</table>

〔註〕:

期刊論文：指在學術性期刊上刊登之文章，其本文部份一般包含引言、方法、結果、及討論，並且一定有參考文獻部分，未在學術性期刊上刊登之文章（研究報告等）與博士或碩士論文，則不包括在內

研討會論文：指參加學術性會議所發表之論文，且尚未在學術性期刊上發表者

專　　著：為對某項學術進行專門性探討之純學術性作品

技術報告：指從事某項技術之創新、設計及製程等研究發展活動所獲致的技術性報告且未公開發表者

技術移轉：指技術由某個單位被另一個單位所擁有的過程。我國目前之技術轉移包括下列三項：一、技術輸入。二、技術輸出。三、技術擴散

技術輸入：藉僑外投資、與外國技術合作、投資國外高科技事業等方式取得先進之技術引進國內者

技術輸出：指直接供應國外買主具生產能力之應用技術、設計、顧問服務及專利等。我國技術輸出方包括整廠輸出、對外投資、對外技術合作及顧問服務等四種

技術擴散：指政府引導式的技術移轉方式，即由財團法人、國營事業或政府研究機構將其開發之技術擴散至民間企業之一種單向移轉（政府移轉民間）

技術創新：指研究執行中產生的技術，且有詳實技術資料文件者

肆、九十三年度計畫重要研究成果

註：群體計畫(PPG)者，不論是否提出各子計畫資料，都必須提出總計畫整合之資料
若為群體計畫，請勾選本表屬於：□子計畫； 或 □總計畫(請自行整合)

※請依下列項目簡述計畫重要之研究成果※

一、 計畫之新發現、新發明或對學術界、產業界具衝擊性（impact）之研究成果。計畫之研究成果，請勾選下列項目並敘述其執行情形。

□ 1.研發或改良國人重要疾病及癌症的早期診斷方式及治療技術
□ 2.發展新的臨床治療方式
□ 3.發展新生物製劑、篩檢試劑及新藥品
□ 4.瞭解常見疾病及癌症之分子遺傳機轉
□ 5.瞭解抗癌藥劑對癌細胞之作用機制
☑ 6.提供有效的疾病預防策略
□ 7.利用生物統計與生物資訊研究，推動台灣生技醫藥研究，促進生物技術與基因體醫學之發展
□ 8.醫療保健政策相關研究
□ 9.瞭解環境毒理機制及重金屬對人體健康的影響
□ 10.研發適合臨床使用的人造器官及生醫材料
□ 11.縮短復健流程並增加復健效果的醫療輔助方式或器材之研究應用
□ 12.改進現有醫療器材的功能或增加檢驗影像的解析能力
□ 13.其他重要疾病或醫藥衛生問題研究_____

臨床報告指出酒精中毒者和酒癮者的健康情形比一般人差，因為這些病患的疾病罹患率及致癌率均比一般人高，這或許和其免疫功能受到抑制有關。本研究結果發現酒精會降低老鼠巨噬細胞數目及其免疫功能。本研究也發現酒精誘導生成的糖皮質素會降低老鼠巨噬細胞數目及其免疫功能。我們使用 RU486（糖皮質素受器的拮抗劑）可讓喝酒老鼠的巨噬細胞數目及其免疫功能部分恢復正常。此研究結果應可應用於人類酒精中毒者之疾病預防。

二、 計畫對民眾具教育宣導之研究成果（此部份將為規劃對一般民眾教育或宣導研究成果之依據，請以淺顯易懂之文字簡述研究成果，內容以不超過 300 字為原則）

本計劃對急性酒精中毒者和酒癮者的健康情形將有重要的幫助，因為這些病患的疾病罹患率及致癌率均比一般人高，這或許和巨噬細胞功能受到

抑制有關。本計劃如以人體作為急性酒精暴露的實驗對象，其研究結果將可直接應用於酒精中毒者和酒癮者之各種治療，包括免疫治療。然而人類個體對酒精的敏感度差異極大，有些人可能千杯不醉，但是有些人可能啜飲少許劑量即導致昏迷而死亡。為了避免意外的發生，本研究以老鼠取代人體作為急性酒精暴露的實驗對象，探討急性酒精暴露對巨噬細胞數目及免疫功能的影響，以作為人類酒精中毒者和酒癮者之免疫治療參考模式。本研究結果發現糖皮質素受器的拮抗劑可讓喝酒老鼠的巨噬細胞數目及其免疫功能部分恢復正常。此研究結果應可應用於人類酒精中毒者之疾病預防。

三、 簡述全程計畫成果之討論與結論，如有技術移轉、技術推廣或業界合作，請概述情形及成效

四、 成效評估（技術面、經濟面、社會面、整合綜效）

酗酒是一個世界性的問題，亞洲國家近年來也漸漸面臨同樣的問題，即使台灣也不例外，雖然目前沒有詳細的流行病學統計，但是酗酒人口顯然較十年前增加許多，而因為酗酒導致器官傷害而住院的病人也越來越多。根據台大醫院 1990 年的統計指出，台灣酒精濫用者佔人口的 5%，酒精依賴者佔人口的 2% 。當時同步參與研究的韓國，其酒精濫用者佔人口的 14%，酒精依賴者佔人口的 9% ； 美國之酒精濫用者佔人口的 8%，酒精依賴者佔人口的 9%（Chen et al., 1990）。行政院衛生署檢疫總所疫情資訊（1998）指出台灣地區成年男性飲酒盛行率達 29%，而且國人飲酒族群有逐漸年輕化的趨勢，台灣青少年飲酒盛行率較四十年前成長數十倍，平均每一百名在學青少年中，十五人有飲酒習慣。另一項調查也指出，高達 26%的酒癮人口在十八歲前已成癮，青少年酗酒問題不容忽視。整體而言，台灣酒癮盛行率由四十年前的 0.15% 增至 15%，成長 100 倍，青少年族群的酗酒率也成長數十倍（周碧瑟，1999）。美國在 1993 年約有一百五十萬的人因酒精的影響而發生了車禍（Anonymous, 1994），而其中有 37% 的人其血液中酒精

的含量高於 0. 2% (Wieczorek et al., 1992)。另根據統計有 44%的美國大學生有急性酒精暴露或中毒的經驗，而有 19% 是經常喝酒的成癮者 (Wechsler et al., 1994)。此急性酒精暴露乃指過去的一星期在一次的場合中喝酒超過 5 杯的劑量。

酒醉即酒精中毒，酒精對大腦的影響很大，大量酒精能麻痺腦部神經，降低大腦皮質之抑制作用，影響判斷力，會出現反應慢、說話含糊的現象，飲酒過量則會造成昏迷。短時間內大量飲酒，最嚴重時則會因酒精抑制延腦的呼吸中樞，造成呼吸的停止，並且也會引起血糖、血壓及體溫下降而造成死亡。先前的研究發現酒精中毒會增加疾病罹患率及罹患癌症的機會，包括上消化道癌（咽、喉、牙齦、口腔、唇及食道癌症）、結腸癌、直腸癌、乳癌、甲狀腺癌、胃癌及胰臟癌 (Baron et al., 1998; Dosemeci et al., 1997; Hayes et al., 1996; Murata et al., 1996; Smith-Warner et al., 1998)。這些因素之一為酒精中毒及因酒精中毒而造成的營養不良，會使身體免疫力降低，進而增加疾病和癌症的罹患率。許多研究已經發現，酒精中毒不僅會抑制淋巴球增生及降低淋巴球數目也會抑制免疫功能，包括抗體反應、巨噬細胞的功能及自然殺手細胞活性進而增加疾病的發生率，例如：呼吸道感染、胃潰瘍、周邊神經病變、肺炎、肺結核、腦膜炎及肝炎 (Caporaso et al., 1991; Chang et al., 2000; Rodriguez-Rodriguez et al., 1995; Singhal et al., 1999)。因此，本計劃的成效評估具多面性，在人類健康上將可帶來莫大的助益。

五、 下年度工作構想及重點之妥適性

本研究結果發現酒精會降低老鼠巨噬細胞數目。我們懷疑是否酒精會促使老鼠巨噬細胞發生細胞凋亡因而降低巨噬細胞的數目。因此，下年度本計劃將探討急性酒精暴露對老鼠腹腔巨噬細胞發生細胞凋亡的影響。我們將進行以下的實驗項目。

1. 以 DAPI 染色法和流式細胞分析儀分析腹腔巨噬細胞發生細胞凋亡的百分比

2. 粒腺體依賴型途徑（mitochondria-dependent pathway）在急性酒精暴露對腹腔巨噬細胞發生細胞凋亡所扮演的角色
3. Fas 受體途徑（Fas receptor-mediated pathway）在急性酒精暴露對腹腔巨噬細胞發生細胞凋亡所扮演的角色
4. MAPK 激脢途徑（MAPK kinase pathway）在急性酒精暴露對腹腔巨噬細胞發生細胞凋亡所扮演的角色

六、 檢討與展望

酗酒已經是一個世界性的問題，而且巨噬細胞又是對抗外來感染及癌症形成的第一道防線，本研究在人類健康上將可帶來莫大的助益。而且這些研究結果，將為未來的研究提供一個重要的啟發。在藥理學的應用上，可研發阻斷內分泌或細胞激素的藥物進而減少對免疫功能的危害，進而達到預防及治療疾病的目的。

伍、九十三年度計畫所培訓之研究人員

註：群體計畫(PPG)者，不論是否提出各子計畫資料，都必須提出總計畫整合之資料
若為群體計畫，請勾選本表屬於：□子計畫；　或　□總計畫(請自行整合)

種類				人數	備註
專任人員	1.	博士後研究人員	訓練中		
			已結訓		
	2.	碩士級研究人員	訓練中		
			已結訓		
	3.	學士級研究人員	訓練中		
			已結訓		
	4.	其他	訓練中		
			已結訓		
兼任人員	1.	博士班研究生	訓練中	1	
			已結訓		
	2.	碩士班研究生	訓練中	1	
			已結訓	1	
醫師			訓練中		
			已結訓		
特殊訓練課程					

註：1.特殊訓練課程請於備註欄說明所訓練課程名稱

2.本表如不敷使用，請自行影印

陸、參與九十三年度計畫所有人力之職級分析

註：群體計畫(PPG)者，不論是否提出各子計畫資料，都必須提出總計畫整合之資料
若為群體計畫，請勾選本表屬於：□子計畫；　或　□總計畫(請自行整合)

職級	所含職級類別	參與人次
第一級	研究員、教授、主治醫師	人
第二級	副研究員、副教授、總醫師、助教授	1人
第三級	助理研究員、講師、住院醫師	人
第四級	研究助理、助教、實習醫師	3人
第五級	技術人員	人
第六級	支援人員	人
合計		4人

〔註〕

第一級：研究員、教授、主治醫師、簡任技正，若非以上職稱則相當於博士滿三年、碩士滿六年、或學士滿九年之研究經驗者

第二級：副研究員、副教授、助研究員、助教授、總醫師、薦任技正，若非以上職稱則相當於博士、碩士滿三年、學士滿六年以上之研究經驗者

第三級：助理研究員、講師、住院醫師、技士，若非以上職稱則相當於碩士、或學士滿三年以上之研究經驗者

第四級：研究助理、助教、實習醫師，若非以上職稱則相當於學士、或專科滿三年以上之研究經驗者

第五級：指目前在研究人員之監督下從事與研究發展有關之技術性工作，且具備下列資格之一者屬之：具初（國）中、高中（職）、大專以上畢業者，或專科畢業目前從事研究發展，經驗未滿三年者

第六級：指在研究發展執行部門參與研究發展有關之事務性及雜項工作者，如人事，會計、秘書、事務人員及維修、機電人員等

柒、參與九十三年度計畫所有人力之學歷分析

註：群體計畫(PPG)者，不論是否提出各子計畫資料，都必須提出總計畫整合之資料
若為群體計畫，請勾選本表屬於: □子計畫； 或 □總計畫(請自行整合)

類別	學歷別	參與人次
1	博士	1人
2	碩士	人
3	學士	人
4	專科	人
5	博士班研究生	1人
6	碩士班研究生	2人
7	其他	人
合計		4人

捌、參與九十三年度計畫之所有協同合作之研究室

群體計畫(PPG)者，不論是否提出各子計畫資料，都必須提出總計畫整合之資料
若為群體計畫，請勾選本表屬於: □子計畫 □總計畫(請自行整合)

機構	研究室名稱	研究室負責人

玖、九十三年度之著作抽印本或手稿

依「貳、九十三年度計畫著作一覽表」所列順序附上文獻抽印本或手稿

Available online at www.sciencedirect.com
SCIENCE DIRECT®
Toxicology Letters 150 (2004) 211–219
Toxicology Letters
www.elsevier.com/locate/toxlet

Increased expression of cytochrome P4501B1 in peripheral leukocytes from lung cancer patients

Ming-Fang Wu[a,b], Wen-Jun Wu[c], Gee-Chen Chang[c,d], Chin-Yi Chen[e], Suh-Woan Hu[f], Wen-Tin Tsai[c], Huei Lee[c], Pinpin Lin[c,*]

[a] *Divisions of Pulmonary Medicine and Medical Oncology, Department of Internal Medicine, Chung Shan Medical University Hospital, Taichung, Taiwan*
[b] *Institute of Medicine, Chung Shan Medical University, Taichung, Taiwan*
[c] *Institute of Toxicology, Chung Shan Medical University, Taichung, Taiwan*
[d] *Division of Pulmonary and Critical Care Medicine, Department of Internal Medicine, Veterans General Hospital-Taichung, Taiwan*
[e] *Department of Thoracic Surgery, Veterans General Hospital-Taichung, Taiwan*
[f] *Institute of Stomatology, Chung Shan Medical University, Taichung, Taiwan*

Received 23 September 2003; received in revised form 20 January 2004; accepted 20 January 2004

Abstract

Aryl hydrocarbon receptor (AhR)-regulated cytochrome P4501A1 (CYP1A1) and P4501B1 (CYP1B1) have been shown to metabolically activate some carcinogens. In the present study, we utilized the real-time reverse transcription-polymerase chain reaction (RT-PCR) assay to compare *AhR*, *CYP1A1* and *CYP1B1* mRNA levels in peripheral leukocytes from 42 lung cancer patients and 59 non-cancer subjects. We found that *CYP1A1* and *CYP1B1* levels, but not *AhR*, were significantly higher in patients than in non-cancer subjects. After stratified by gender, *CYP1A1* levels were significantly higher in female patients than in female controls. After controlling for age, smoking status and gender, lung cancer patients were more likely to be *CYP1B1* high expressers ($P < 0.05$). Neither *AhR* nor *CYP1A1* levels was associated with lung cancer incidence. Leu–Val polymorphism of *CYP1B1* was not associated with lung cancer risk in our study. These data indicated that *CYP1B1* mRNA levels were elevated in peripheral leukocytes of lung cancer patients.

Keywords: Aryl hydrocarbon receptor; Cytochrome P4501A1; Cytochrome P4501B1; Lung cancer

1. Introduction

Cytochrome P4501A1 (CYP1A1) and P4501B1 (CYP1B1) have been shown to participate in metabolic activation of exogenous and endogenous carcinogens, such as polycyclic aromatic hydrocarbons (PAH) and estrogens. CYP1A1 and CYP1B1 respectively hydrolyze 17β-estradiol to 2-hydroxylated and 4-hydroxylated estradiol (Cavalieri et al., 2000). 4-Hydroxylated estradiol was demonstrated to be carcinogenic in hamsters (Liehr et al., 1986). Therefore, CYP1A1 and CYP1B1 activity in tissues may affect their responsiveness to certain chemical carcinogens.

* Corresponding author. Tel.: +886-42473-0022; fax: +886-42475-1101.
E-mail address: ppl@csmu.edu.tw (P. Lin).

0378-4274/$ – see front matter © 2004 Elsevier Ireland Ltd. All rights reserved.
doi:10.1016/j.toxlet.2004.01.006

CYP1A1 and CYP1B1 not only metabolically activate PAH, but also are induced by PAH and dioxins (Whitlock, 1999). PAH and dioxins activate aryl hydrocarbon receptor (AhR) and subsequently increase CYP1A1 and CYP1B1 gene expression (Kress and Greenlee, 1997; Whitlock, 1999). Several lines of evidence showed that AhR activation was required for PAH and dioxin-induced carcinogenesis or toxicities in mice (Fernandez-Salguero et al., 1996; Nebert, 1989; Shimizu et al., 2000). PAH and dioxins are important carcinogens found in air pollutants (Shimada et al., 1992, 1996). Heavy exposure to PAH or dioxins contaminated air pollutants has been associated with the increased risk of lung cancer (Boffetta et al., 1997; Kogevinas, 2000). Therefore, AhR-mediated CYP1A1 and 1B1 expression is crucial for PAH or dioxin-associated lung cancer.

CYP1A1 inducibility was suggested to be a susceptibility biomarker for lung cancer. Jacquet et al. (1997) showed that CYP1A1 inducibility in lymphocytes correlated with that in lungs. Some studies showed that CYP1A1 inducibility in lymphocytes from lung cancer patients was significantly higher than those from healthy subjects (Kellermann et al., 1973; Kiyohara et al., 1998). However, the relationship between CYP1A1 inducibility and lung cancer risk is still controversial (Prasad et al., 1979; Ward et al., 1978). Unlike CYP1A1, the information on the relationship between CYP1B1 and lung cancer risk is still very limited. *CYP1B1* gene expression was constitutively detectable and inducible by PAH and dioxin in lung cells and peripheral lymphocytes (Chang et al., 1999; Lin et al., 2003b; Spencer et al., 1999). Watanabe et al. (2000) demonstrated that *CYP1B1* polymorphism was significantly associated with the incidence of squamous cell carcinoma of the lung. This suggests that CYP1B1 polymorphism associated alteration in CYP1B1 activity may affect lung carcinogenesis. Recently, our and Spivack's studies (Lin et al., 2003a; Spivack et al., 2001) showed that CYP1B1 protein was constitutively expressed in normal lung tissues and lung tumors. However, it is still unclear whether individual variation in CYP1B1 activity or expression plays a role in the development of lung cancer.

Since AhR regulates CYP1A1 induction, it is plausible to propose a positive correlation between AhR expression and CYP1A1 inducibility. Recently, we successfully demonstrated this correlation occurred in peripheral lymphocytes from healthy subjects (Lin et al., 2003b). If CYP1A1 inducibility in lymphocytes is a susceptibility factor for lung cancer, we expect that AhR expression should be higher in lymphocytes from lung cancer patients than those from healthy individuals. We also found that CYP1B1 expression correlated with AhR expression in lymphocytes (Lin et al., 2003b). Therefore, it is worthwhile to investigate whether expression of AhR and AhR-regulated genes was increased in peripheral leukocytes of lung cancer patients.

Recently, we developed the real-time reverse transcription-polymerase chain reaction (RT-PCR) assay to quantify relative mRNA levels of *CYP1A1*, CYP1B1 and *AhR* in peripheral lymphocytes (Lin et al., 2003b). In the present study, we quantified and compared relative mRNA levels of *CYP1A1*, *CYP1B1* and *AhR* in peripheral leukocytes from 42 lung cancer patients and 59 healthy subjects with the real-time quantitative RT-PCR assay. We believe that the results of our present investigation will serve to further elucidate the relationship between *CYP1A1*, *CYP1B1* and *AhR* expression and lung cancer incidence in humans.

2. Materials and methods

2.1. Study population

Controls were non-cancer individuals who attended a health status examination at Veterans General Hospital-Taichung. Patients were those who attended the Clinics at Chung Shan Medical University Hospital or Veterans General Hospital-Taichung. The histologies of lung cancer tumor types were determined according to the WHO classification. Study subjects were interviewed and asked about occupation and smoking status. Smokers were those had history of cigarette smoking for at least 1 year. The average smoking pack-year for control smokers was 600 (75–1000). However, the information of pack-year for patients was not available. Non-smokers were never-smokers. Blood was collected from lung cancer patients prior to any treatment. A total of 42 lung cancer patients were recruited, including 22 adenocarcinomas, 14 squamous cell carcinomas, 4

small cell lung cancers and 2 large cell lung cancers. This project was approved by the Human Subjects Committee in Chung Shan Medical University Hospital.

2.2. Quantitative real-time reverse transcription-polymerase chain reaction assay

Three milliliters of peripheral blood was collected from each subject. Total RNAs of blood were prepared by TRIzol® Reagent (Life Technologies, Rockville, MD) and the phenol–chloroform extraction method. Synthesis of cDNA was done with 3 μg total RNA using M-MLV Reverse Transcriptase (Promega, Madison, WI) and 200 pmol/μl random primer (New England BioLabs® Inc.). Quantitative PCR was performed using the QuantiTect SYBR Green PCR kit (Qiagen, Hilden, Germany) and analyzed on an ABI PRISM 7700 Sequence Detector System (Perkin-Elmer Applied Biosystem, Foster City, CA). Primers were chosen with the assistance of the computer program—Primer Express™ 1.5 (Perkin-Elmer Applied Biosystem, Foster City, CA). To avoid amplification of contaminating genomic DNA, one of the two primers was placed at the junction between two exons. *AhR* primers were 5′-acatcacctacgccagtcgc and 5′-tctatgccgcttggaaggat. *CYP1B1* primers were 5′-gctgcagtggctgctcct and 5′-cccacgacctgatccaattct. *CYP1A1* primers were 5′-caccatcccccacagcac and 5′-acaaagacacaacgcccctt. *18S rRNA* primers were 5′-ttaagtccctgccctttgtacac and 5′-cgatccgagggcctcact. The optimal primer concentrations for *AhR*, *CYP1B1*, *CYP1A1*, and *18S rRNA* were 400, 200, 200 and 100 nM, respectively. The thermal cycling comprised an initial step at 50 °C for 2 min, followed by a denaturation step at 95 °C for 10 min, 40 cycles at 95 °C for 15 s and 40 cycles at 60 °C for 1 min. Varying lengths of oligonucleotides produce dissociation peaks at different melting temperatures. Consequently, at the end of the PCR cycles, the PCR products were analyzed using heat dissociation protocol to confirm that one single PCR product was detected by SYBR Green dye. Each data point was repeated at least twice. Quantitative values were obtained from the threshold PCR cycle number (Ct) at which the increase in signal associated with an exponential growth for PCR product starts to be detected. The *AhR*, *CYP1A1* and *CYP1B1* mRNA levels in each sample were normalized to its *18S rRNA* content. The relative mRNA levels of the target gene: $2^{-\Delta Ct}$, $\Delta Ct = Ct_{\text{target gene}} - Ct_{\text{18S rRNA}}$.

2.3. CYP1B1 genotyping

Genotyping of the CYP1B1 polymorphism Leu432Val was performed by a two-step, allele-specific PCR method (Aklillu et al., 2002). In the first PCR reaction, a 270 bp PCR product containing the polymorphic site was amplified with the primers, tatgaagccatgcgcttctc and aagttcttcgccaatgcacc, in the following condition: denaturation at 95 °C for 1 min, followed by 35 cycles at 95 °C for 15 s, at 58 °C for 40 s, and at 72 °C for 1 min, and final extension for 72 °C for 7 min. The first PCR product was subsequently used as a template in second PCR reaction with the forward primer, tatgaagccatgcgcttctc, and the allele-specific primer, gttaggccacttcag for Leu allele or gttaggccacttcac for Val allele, in the following condition: denaturation at 95 °C for 1 min, followed by 18 cycles at 95 °C for 15 s, at 60 °C for 30 s, and at 72 °C for 45 s, and final extension for 72 °C for 7 min. The second PCR product was 153 bp. The genotypes were determined by the formation of second PCR product. All Leu/Val and Val/Val genotypes in our samples were confirmed with direct DNA sequencing.

2.4. Statistical analysis

Comparisons of smoking status and gender between the patient and control groups were done by χ^2-test. Age in the two groups was compared with Student's *t*-test. Relative mRNA levels were compared with Mann–Whitney *U*-test. After stratifying all study subjects into high or low gene expressers by the median of respective mRNA levels, frequencies of high and low gene expressers in the patient and control groups were compared with the χ^2-test. Finally, the logistic regression analysis was performed to assess the associations between lung cancer incidence and *AhR*, *CYP1A1* and *CYP1B1 mRNA* levels (high versus low) or CYP1B1 genotypes (*Leu/Val* + *Val/Val* versus *Leu/Leu*), respectively, controlling for age, gender and smoking status. An alpha-level of 0.05 was used for all statistical tests. SPSS software (SPSS Inc., Chicago, IL, Version 6.0) was applied for the data analysis.

Table 1
Characteristics of lung cancer patients and control subjects

	Patients	Controls	*P* value
Subject numbers	42	59	
Age, mean ± S.D. (years)	63 ± 10	57 ± 5	<0.01[a]
Gender (%)			
Male	71.4	50.8	0.04[b]
Female	28.6	49.2	
Smoking status (%)			
Smokers	52.4	18.6	<0.01[b]
Non-smokers	47.6	81.4	

[a] Analyzed with students' *t*-test.
[b] Analyzed with χ^2-test.

3. Results

A total of 42 lung cancer patients and 59 non-cancer subjects were recruited in this study. The average age was greater in the patient group than in the control group (Table 1). The proportion of males was significantly higher in the patient group than in the control group (Table 1). Cigarette smoking was more common in the patient group than in the control group (Table 1). Among patients, approximately 68% (15/22) and 18% (4/22) of blood samples from smokers were respectively collected within 70 days and 71–141 days after they were diagnosed. *AhR*, *CYP1A1* and *CYP1B1* mRNA were detectable but highly variable in peripheral leukocytes (Fig. 1). *AhR* and *CYP1B1* levels had approximately a 100-fold variation among these subjects. In some subjects, *CYP1A1* levels were extremely low and inter-individual variation of *CYP1A1* levels was more than a 1000-fold. *CYP1A1* and *CYP1B1* levels were significantly higher in lung cancer patients than in non-cancer subjects (Fig. 1, $P < 0.01$). However, *AhR* levels were similar between the patient and control groups (Fig. 1).

After stratified by smoking behavior, *CYP1B1* levels were still significantly higher in patients than in controls among smokers and non-smokers (Table 2). When groups were stratified by gender, *CYP1B1* levels

Table 2
Stratification of gene expression levels by smoking status, gender or age[a]

	n[b]	*AhR*[c]	*CYP1B1*[c]	*CYP1A1*[c]
Smokers				
Patients	22	5925.34 ± 2076.23	17196.04 ± 3350.43**	13.04 ± 4.25
Controls	11	2299.95 ± 613.95	4692.23 ± 975.45	6.22 ± 1.53
Non-smokers				
Patients	20	3000.61 ± 768.48	16003.78 ± 2510.67**	11.83 ± 4.24
Controls	48	1654.01 ± 167.74	5912.02 ± 1407.54	2.39 ± 0.49
Males				
Patients	30	5620.36 ± 1579.75	18031.12 ± 2762.63**	13.70 ± 3.92
Controls	30	1830.95 ± 266.67	6342.23 ± 2190.36	3.53 ± 0.71
Females				
Patients	12	1813.24 ± 277.41	13121.23 ± 2383.31**	9.37 ± 3.55*
Controls	29	1715.98 ± 239.59	5004.30 ± 690.48	2.66 ± 0.77
≤59 years old				
Patients	12	2242.88 ± 843.15	15366.87 ± 3395.93**	6.92 ± 3.55
Controls	39	1418.09 ± 168.89	6038.56 ± 1709.03	1.90 ± 0.38
>59 years old				
Patients	30	5448.50 ± 1562.37	17132.86 ± 2636.47**	14.68 ± 3.86
Controls	20	2469.31 ± 369.19	4906.65 ± 795.68	5.45 ± 1.21

[a] Analyzed with Mann–Whitney *U*-test.
[b] Subject numbers.
[c] Specific gene molecules per 10^7 molecules of 18S rRNA were presented as mean ± S.D.
* $P < 0.05$.
** $P < 0.01$.

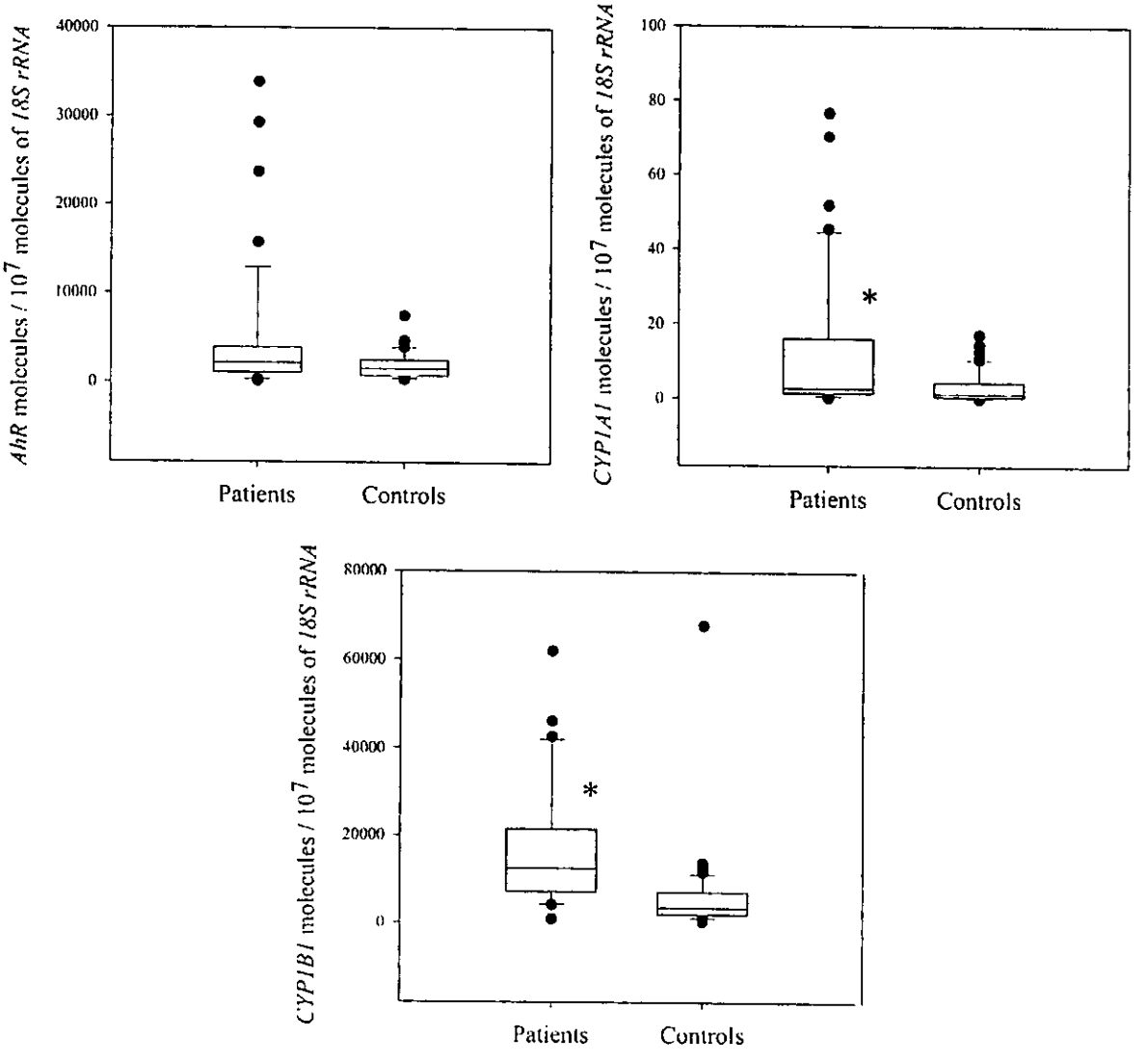

Fig. 1. Distribution of *AhR*, *CYP1A1* and *CYP1B1* levels in peripheral leukocytes from patients and controls. Relative expression levels of *AhR*, *CYP1A1* and *CYP1B1* were determined as previously described in Section 2. Gene expression levels between patients and controls were compared with Mann–Whitney *U*-test. $^{*}P < 0.01$.

were significantly higher in both male and female patients than in corresponding controls (Table 2). Among females, *CYP1A1* levels were significantly higher in patients than in controls (Table 2). After stratified by age, *CYP1B1* levels were significantly higher in both elder and younger patients than in corresponding controls (Table 2). Regardless of stratification by smoking status, gender or age, *AhR* levels were similar between patients and controls (Table 2).

Since *AhR*, *CYP1B1* and *CYP1A1* levels in leukocytes were highly variable, we divided each group into high or low expressers according to *AhR*, *CYP1B1* or *CYP1A1* levels. The medians of gene expression levels were used as the thresholds to define low versus high expressers. Then we evaluated the association between *AhR*, *CYP1A1* or *CYP1B1* levels and lung cancer incidence with the logistic regression analysis. After age, smoking status and gender were controlled in

Table 3
Logistic regression analysis for the association between gene expression levels and lung cancer[a]

Gene expression levels	n^b (patients/controls)
AhR	
Low	17/34
High	25/25
CYP1A1	
Low	15/36
High	27/23
*CYP1B1**	
Low	8/43
High	34/16

[a] Adjusted for age, gender and smoking status.
[b] Subject numbers.
* $P < 0.05$.

the analysis, neither *AhR* nor *CYP1A1* levels was associated with lung cancer incidence (Table 3). High *CYP1B1* expressers were significantly more prevalent in lung cancer patients (Table 3).

CYP1B1 Leu–Val genotypes were determined among 42 lung cancer patients and 58 control subjects. The proportions of wild-type *CYP1B1* (Leu/Leu) were 73.8% (31/42) and 75.9% (44/58) in the patient and control groups, respectively (Table 4). The association between *CYP1B1* genotypes and lung cancer risk was also evaluated with the logistic regression analysis. After controlling for age, smoking status and gender, *CYP1B1* genotypes have no association with lung cancer risk in this study (Table 4).

4. Discussion

AhR mediated CYP1A1 and CYP1B1 expression has been implied to play a role in exogenous or endogenous carcinogen-induced lung cancer. In the present study, we found that *CYP1A1* and *CYP1B1* levels, but not *AhR*, were significantly higher in peripheral leukocytes from lung cancer patients than those from controls. But after controlling for gender, age and smoking status, patients were only more prone to be *CYP1B1* high expressers.

CYP1B1 has been shown to involve in metabolic activation of some endogenous and exogenous carcinogens, such as 17β-estradiol, 7,12-dimethylbenz[*a*]anthracene, and 1-nitropyrene (Cavalieri et al., 2000; Hatanaka et al., 2001; Shimada et al., 1996). One-nitropyrene, present in automobile exhaust (Yamazaki et al., 2000), has been demonstrated to induce lung tumors in animal studies (Moon et al., 1990). CYP1B1 protein was constitutively expressed in normal lungs (Lin et al., 2003a; Spivack et al., 2001). Assuming *CYP1B1* expression in peripheral leukocytes correlates with that in lung tissues, individuals with high *CYP1B1* expression in peripheral leukocytes would have higher metabolic activation capability for certain carcinogens in lungs. Increased *CYP1B1* expression in peripheral leukocytes from lung cancer patients suggested that CYP1B1 might involve in the development of lung cancer.

Previously we demonstrated that CYP1B1 expression positively correlated with AhR expression in lung tumors (Lin et al., 2003a). We proposed that endogenous AhR ligands was released or increased to up-regulate CYP1B1 in patients with high AhR expression (Lin et al., 2003a). In the present study, *CYP1B1* mRNA levels were significantly higher in peripheral leukocytes from lung cancer patients than from non-cancer subjects. *AhR* levels was similar between cases and controls, although *AhR* expression positively correlated with *CYP1B1* expression (data not shown). These findings implied that unknown AhR ligands might be released to systemically increase CYP1B1 expression in peripheral leukocytes

Table 4
Logistic regression analysis for the association between CYP1B1 genotypes and lung cancer

CYP1B1 genotypes	n^a (patients/controls)	OR (95% CI[b])	OR (95% CI[c])
Leu/Leu	31/44	1.00	1.00
Leu/Val + *Val/Val*	11/14	1.12 (0.48–2.78)	1.41 (0.49–4.00)

[a] Subject numbers.
[b] Crude OR: odds ratio; 95% CI: 95% confidence interval.
[c] OR and 95% CI after adjusted for age, gender and smoking status.

of lung cancer patients. Ligand-independent AhR activation was reported under certain circumstances (Ma and Whitlock, 1996). Therefore, it is also possible that AhR was constitutively activated in lung cancer patients, which subsequently increased CYP1B1 mRNA levels.

We also cannot rule out the possibility that increased CYP1B1 mRNA levels in lung cancer patients is a dietary AhR ligand-induced, environmental pollutant-induced or inherited phenotype. A variety of naturally occurring dietary chemicals, such as flavonoids, have been characterized as AhR ligands or agonists (Denison and Nagy, 2003). Uptake of foods containing high levels of AhR ligands may increase CYP1B1 expression. Dioxin is the most potent AhR agonist. Toide et al. (2003) demonstrated that *CYP1B1*, but not *CYP1A1*, mRNA levels in leukocytes were significantly correlated with the plasma concentrations of dioxins among a dioxin high exposure group. It suggested that exposure to high levels of dioxins might increase *CYP1B1* mRNA levels in peripheral leukocytes. Genetic polymorphism may contribute to individual variation of *CYP1B1* expression. Several genetic polymorphisms were identified in *CYP1B1* gene, but their relationship with *CYP1B1* expression levels was still unclear. Some studies indicated that Leu432 variants of CYP1B1 showed higher rate of oxidation of benzo[a]pyrene (BaP) and 4-hydroxylation of 17β-estradiol (Shimada et al., 1999, 2001). The Val allele frequency of *CYP1B1* polymorphism in the present study was similar to that in a Japanese population (Inoue et al., 2000). In our study, we failed to observe the association between *CYP1B1* expression and Leu/Val polymorphism. Furthermore, no correlation between *CYP1B1* expression and genotypes was found in our study (data not shown). It is likely that a larger population is needed to assess the association of *CYP1B1* genotypes with *CYP1B1* expression or lung cancer risk.

PAH is one of the major carcinogens found in cigarette smoke (Hecht, 1999). Cigarette smoke condensate was demonstrated to induce CYP1A1 expression and activity in vitro and in vivo (Dertinger et al., 2001). We also reported that BaP, the major PAH present in cigarette smoke (Hecht, 1999), induced *CYP1A1* and *CYP1B1* mRNA levels in human lung cells (Chang et al., 1999). Furthermore, *CYP1A1* inducibility by PAH in peripheral leukocytes was much higher than *CYP1B1* inducibility (Lin et al., 2003b). However, in our present study, we only observed a slightly higher *CYP1A1* levels in healthy smokers than in healthy non-smokers. *CYP1B1* levels were similar between healthy smokers and non-smokers. It is likely that cigarette smoke-induced *CYP1A1* and *CYP1B1* mRNA levels in peripheral leukocytes was interfered by several factors, such as half-life of CYP1A1 induction, CYP1A1 genotypes and the duration between active smoking and sampling of blood. For example, patients with lung cancers are advised to cease cigarette smoking from time of diagnosis. The cessation of active smoking may lessen the influence of cigarette smoking on *CYP1A1* and *CYP1B1* expression.

Several epidemiological studies have indicated that female smokers were at higher risk of lung cancer than male smokers (Prescott et al., 1998; Zang and Wynder, 1996). It was further supported by Mollerup et al.'s (1999) findings that levels of aromatic/hydrophobic DNA adducts and *CYP1A1* expression levels were higher in non-tumor lung tissues from female than those from male smokers. Although majority of female lung cancer patients were non-smokers in Taiwan, our present study showed that both *CYP1A1* and *CYP1B1* levels were significantly higher in female patients than controls. Estrogen metabolites are considered to be responsible for estrogen-induced carcinogenesis (Cavalieri et al., 2000). CYP1A1 and CYP1B1 catalyzed hydroxylated estradiols were demonstrated to convert into quinones which formed DNA adducts (Convert et al., 2002). These data supported the hypothesis that CYP1A1 and CYP1B1 might contribute to the development of female lung cancer.

Over-expressed in variety of tumors, including lung tumors, CYP1B1 has been implied as a marker for tumor diagnosis (Chang and Puga, 1998; Crawford et al., 1997; Murray et al., 1997). If metastasis occurs in the tumors, tumor cells with high CYP1B1 expression might be detected in peripheral leukocytes. In our lung cancer patients, 18 of 44 patients were involved with lymph node metastases. But high *CYP1B1* expression in peripheral leukocytes was not associated with metastasis among these patients (data not shown). Thus, high CYP1B1 expression in peripheral leukocytes was not resulted from tumor cells in the circulation system.

AhR and *CYP1A1* levels tended to be higher in patients than controls, although it was not statistically significant. The small sample size might be a problem. In the future, we had like to increase the sample numbers to study the relationship between *AhR*, *CYP1A1* expression and lung cancer incidence.

Acknowledgements

This work was supported by the National Science Council of the ROC under Grant Number NSC 92-2320-B-040-033, by the Veterans General Hospital-Taichung of the ROC under grant number TCVGH-917320D and by Phillip Morris External Research Program.

References

Aklillu, E., Oscarson, M., Hidestrand, M., Leidvik, B., Otter, C., Ingelman-Sundberg, M., 2002. Functional analysis of six different polymorphic CYP1B1 enzyme variants found in an Ethiopian population. Mol. Pharmacol. 61, 586–594.

Boffetta, P., Jourenkova, N., Gustavsson, P., 1997. Cancer risk from occupational and environmental exposure to polycyclic aromatic hydrocarbons. Cancer Causes Contr. 8, 444–472.

Cavalieri, E., Frenkel, K., Liehr, J.G., Rogan, E., Roy, D., 2000. Estrogens as endogenous genotoxic agents—DNA adducts and mutations. J. Natl. Cancer Inst. Monogr. 27, 75–93.

Chang, C.Y., Puga, A., 1998. Constitutive activation of the aromatic hydrocarbon receptor. Mol. Cell Biol. 18, 525–535.

Chang, K.W., Lee, H., Wang, H.J., Chen, S.Y., Lin, P., 1999. Differential response to benzo[A]pyrene in human lung adenocarcinoma cell lines: the absence of aryl hydrocarbon receptor activation. Life Sci. 65, 1339–1349.

Convert, O., Van Aerden, C., Debrauwer, L., Rathahao, E., Molines, H., Fournier, F., Tabet, J.C., Paris, A., 2002. Reactions of estradiol-2,3-quinone with deoxyribonucleosides: possible insights in the reactivity of estrogen quinones with DNA. Chem. Res. Toxicol. 15, 754–764.

Crawford, R.B., Holsapple, M.P., Kaminski, N.E., 1997. Leukocyte activation induces aryl hydrocarbon receptor up-regulation, DNA binding, and increased Cyp1a1 expression in the absence of exogenous ligand. Mol. Pharmacol. 52, 921–927.

Denison, M.S., Nagy, S.R., 2003. Activation of the aryl hydrocarbon receptor by structurally diverse exogenous and endogenous chemicals. Annu. Rev. Pharmacol. Toxicol. 43, 309–334.

Dertinger, S.D., Nazarenko, D.A., Silverstone, A.E., Gasiewicz, T.A., 2001. Aryl hydrocarbon receptor signaling plays a significant role in mediating benzo[a]pyrene- and cigarette smoke condensate-induced cytogenetic damage in vivo. Carcinogenesis 22, 171–177.

Fernandez-Salguero, P.M., Hilbert, D.M., Rudikoff, S., Ward, J.M., Gonzalez, F.J., 1996. Aryl-hydrocarbon receptor-deficient mice are resistant to 2,3,7,8-tetrachlorodibenzo-*p*-dioxin-induced toxicity. Toxicol. Appl. Pharmacol. 140, 173–179.

Hatanaka, N., Yamazaki, H., Oda, Y., Guengerich, F.P., Nakajima, M., Yokoi, T., 2001. Metabolic activation of carcinogenic 1-nitropyrene by human cytochrome P450 1B1 in *Salmonella typhimurium* strain expressing an *O*-acetyltransferase in SOS/umu assay. Mutat. Res. 497, 223–233.

Hecht, S.S., 1999. Tobacco smoke carcinogens and lung cancer. J. Natl. Cancer Inst. 91, 1194–1210.

Inoue, K., Asao, T., Shimada, T., 2000. Ethnic-related differences in the frequency distribution of genetic polymorphisms in the CYP1A1 and CYP1B1 genes in Japanese and Caucasian populations. Xenobiotica 30, 285–295.

Jacquet, M., Lambert, V., Todaro, A., Kremers, P., 1997. Mitogen-activated lymphocytes: a good model for characterising lung CYP1A1 inducibility. Eur. J. Epidemiol. 13, 177–183.

Kellermann, G., Shaw, C.R., Luyten-Kellerman, M., 1973. Aryl hydrocarbon hydroxylase inducibility and bronchogenic carcinoma. N. Engl. J. Med. 289, 934–937.

Kiyohara, C., Nakanishi, Y., Inutsuka, S., Takayama, K., Hara, N., Motohiro, A., Tanaka, K., Kono, S., Hirohata, T., 1998. The relationship between CYP1A1 aryl hydrocarbon hydroxylase activity and lung cancer in a Japanese population. Pharmacogenetics 8, 315–323.

Kogevinas, M., 2000. Studies of cancer in humans. Food Addit. Contam. 17, 317–324.

Kress, S., Greenlee, W.F., 1997. Cell-specific regulation of human CYP1A1 and CYP1B1 genes. Cancer Res. 57, 1264–1269.

Liehr, J.G., Fang, W.F., Sirbasku, D.A., Ari-Ulubelen, A., 1986. Carcinogenicity of catechol estrogens in Syrian hamsters. J. Steroid Biochem. 24, 353–356.

Lin, P., Chang, H., Ho, W.L., Wu, M.-H., Su, J.-M., 2003a. Association of aryl hydrocarbon receptor and cytochrome P4501B1 expressions in human non-small cell lung cancers. Lung Cancer 42, 255–261.

Lin, P., Hu, S.W., Chang, T.H., 2003b. Correlation between gene expression of aryl hydrocarbon receptor (AhR), hydrocarbon receptor nuclear translocator (Arnt), cytochromes P4501A1 (CYP1A1) and 1B1 (CYP1B1), and inducibility of CYP1A1 and CYP1B1 in human lymphocytes. Toxicol. Sci. 71, 20–26.

Ma, Q., Whitlock Jr., J.P., 1996. The aromatic hydrocarbon receptor modulates the Hepa 1c1c7 cell cycle and differentiated state independently of dioxin. Mol. Cell Biol. 16, 2144–2150.

Mollerup, S., Ryberg, D., Hewer, A., Phillips, D.H., Haugen, A., 1999. Sex differences in lung CYP1A1 expression and DNA adduct levels among lung cancer patients. Cancer Res. 59, 3317–3320.

Moon, R.C., Rao, K.V., Detrisac, C.J., 1990. Respiratory carcinogenesis of nitroaromatics. Res. Rep. Health Eff. Inst. 32, 1–29.

Murray, G.I., Taylor, M.C., McFadyen, M.C., McKay, J.A., Greenlee, W.F., Burke, M.D., Melvin, W.T., 1997. Tumor-specific expression of cytochrome P450 CYP1B1. Cancer Res. 57, 3026–3031.

Nebert, D.W., 1989. The Ah locus: genetic differences in toxicity, cancer, mutation, and birth defects. Crit. Rev. Toxicol. 20, 153–174.

Prasad, R., Prasad, N., Harrell, J.E., Thornby, J., Liem, J.H., Hudgins, P.T., Tsuang, J., 1979. Aryl hydrocarbon hydroxylase inducibility and lymphoblast formation in lung cancer patients. Int. J. Cancer 23, 316–320.

Prescott, E., Osler, M., Hein, H.O., Borch-Johnsen, K., Lange, P., Schnohr, P., Vestbo, J., 1998. Gender and smoking-related risk of lung cancer. the Copenhagen center for prospective population studies. Epidemiology 9, 79–83.

Shimada, T., Hayes, C.L., Yamazaki, H., Amin, S., Hecht, S.S., Guengerich, F.P., Sutter, T.R., 1996. Activation of chemically diverse procarcinogens by human cytochrome P-450 1B1. Cancer Res. 56, 2979–2984.

Shimada, T., Watanabe, J., Inoue, K., Guengerich, F.P., Gillam, E.M., 2001. Specificity of 17beta-oestradiol and benzo[a]pyrene oxidation by polymorphic human cytochrome P4501B1 variants substituted at residues 48, 119 and 432. Xenobiotica 31, 163–176.

Shimada, T., Watanabe, J., Kawajiri, K., Sutter, T.R., Guengerich, F.P., Gillam, E.M., Inoue, K., 1999. Catalytic properties of polymorphic human cytochrome P450 1B1 variants. Carcinogenesis 20, 1607–1613.

Shimada, T., Yun, C.H., Yamazaki, H., Gautier, J.C., Beaune, P.H., Guengerich, F.P., 1992. Characterization of human lung microsomal cytochrome P-450 1A1 and its role in the oxidation of chemical carcinogens. Mol. Pharmacol. 41, 856–864.

Shimizu, Y., Nakatsuru, Y., Ichinose, M., Takahashi, Y., Kume, H., Mimura, J., Fujii-Kuriyama, Y., Ishikawa, T., 2000. Benzo[a]-pyrene carcinogenicity is lost in mice lacking the aryl hydrocarbon receptor. Proc. Natl. Acad. Sci. U.S.A. 97, 779–782.

Spencer, D.L., Masten, S.A., Lanier, K.M., Yang, X., Grassman, J.A., Miller, C.R., Sutter, T.R., Lucier, G.W., Walker, N.J., 1999. Quantitative analysis of constitutive and 2378-tetrachlorodibenzo-*p*-dioxin-induced cytochrome P450 1B1 expression in human lymphocytes. Cancer Epidemiol. Biomarkers Prev. 8, 139–146.

Spivack, S.D., Hurteau, G.J., Reilly, A.A., Aldous, K.M., Ding, X., Kaminsky, L.S., 2001. CYP1B1 expression in human lung. Drug Metab. Dispos. 29, 916–922.

Toide, K., Yamazaki, H., Nagashima, R., Itoh, K., Iwano, S., Takahashi, Y., Watanabe, S., Kamataki, T., 2003. Aryl hydrocarbon hydroxylase represents CYP1B1, and not CYP1A1, in human freshly isolated white cells: trimodal distribution of Japanese population according to induction of CYP1B1 mRNA by environmental dioxins. Cancer Epidemiol. Biomarkers Prev. 12, 219–222.

Ward, E., Paigen, B., Steenland, K., Vincent, R., Minowada, J., Gurtoo, H.L., Sartori, P., Havens, M.B., 1978. Aryl hydrocarbon hydroxylase in persons with lung or laryngeal cancer. Int. J. Cancer 22, 384–389.

Watanabe, J., Shimada, T., Gillam, E.M., Ikuta, T., Suemasu, K., Higashi, Y., Gotoh, O., Kawajiri, K., 2000. Association of CYP1B1 genetic polymorphism with incidence to breast and lung cancer. Pharmacogenetics 10, 25–33.

Whitlock Jr., J.P., 1999. Induction of cytochrome P4501A1. Annu. Rev. Pharmacol. Toxicol. 39, 103–125.

Yamazaki, H., Hatanaka, N., Kizu, R., Hayakawa, K., Shimada, N., Guengerich, F.P., Nakajima, M., Yokoi, T., 2000. Bioactivation of diesel exhaust particle extracts and their major nitrated polycyclic aromatic hydrocarbon components, 1-nitropyrene and dinitropyrenes, by human cytochromes P450 1A1, 1A1, and 1B1. Mutat. Res. 472, 129–138.

Zang, E.A., Wynder, E.L., 1996. Differences in lung cancer risk between men and women: examination of the evidence. J. Natl. Cancer Inst. 88, 183–192.

Scand J Infect Dis 36: 570–577, 2004

Taylor & Francis
healthsciences

Human Parvovirus B19 Non-structural Protein (NS1) Induces Apoptosis through Mitochondria Cell Death Pathway in COS-7 Cells

TSAI-CHING HSU[1,2,3], WEN-JUN WU[4], MENG-CHI CHEN[2] and GREGORY J. TSAY[1,2]

From the [1]Department of Medicine, and Institutes of [2]Immunology, [3]Medicine, and [4]Toxicology, Chung Shan Medical University, Taichung, Taiwan

Human parvovirus B19 has been found in various tissues in addition to erythroid lineage cells, and non-structural protein (NS1) is reported to induce cytotoxicity and apoptosis in erythroid lineage cells, but the mechanism in non-permissive cells is still unclear. To address this issue, we have constructed the NS1 gene in a cytomegalovirus episomal vector, pEGFP-C1 and transfected it into monkey epithelial cells, COS-7. EGFP-NS1 expression in transfected cells was monitored and assessed by fluorescence microscopy, RT-PCR and Western blot. The flow cytometric analysis showed that the NS1-transfected cells were arrested at G1 phase by paclitaxel treatment and there was increased apoptosis. The expression of p53, an important molecule in apoptosis and cell cycle regulation, and its downstream cell cycle kinase inhibitors $p16^{INK4}$ and $p21^{WAF1/CIP1}$ were up-regulated in the NS1-transfected cells. Also, increased expression of the pro-apoptotic Bcl-2 members Bax, Bad and activation of caspase 3 and caspase 9, but not the activation of caspase 8 or Fas were detected in the NS1-transfected cells. p53-induced Bax expression and subsequent activation of caspase 9 is probably the apoptotic pathway in NS1-transfected cells since activation of the caspase 9 was suppressed by the p53 inhibitor and apoptosis was significantly inhibited by the caspase 9 inhibitor. Our results suggest that the cell death of the NS1-transfected cells is associated with mitochondria related apoptosis. These findings might provide alternative information for further study and characterization of B19 NS1 protein in B19 non-permissive cells.

G. J. Tsay, Department of Medicine and Institute of Immunology, Chung Shan Medical University, 110 Sec.1, Chien Kuo N. Road, Taichung 402, Taiwan (Tel. +886 4 2473 0022 ext 1705, fax. +886 4 2324 8172, e-mail. gjt@csmu.edu.tw)

INTRODUCTION

Human parvovirus B19 (B19) was discovered in 1975 (1) and has been associated with a variety of clinical manifestations, including rash, thrombocytopenia, leukopenia, fetal wastage, hypocomplementemia, autoimmune hemolytic anemia, arthritis and vasculitis (2–4). It is the causative agent in erythema infectiosum (EI). Additionally, B19 infection is associated with elevated levels of antinuclear antibody (ANA), anti-double stranded DNA antibody (anti-dsDNA), anti-neutrophil cytoplasmic antibodies (ANCA), and anti-cardiolipin antibodies (aCL) (5, 6). The association of B19 infection with autoimmune diseases, including systemic lupus erythematosus (SLE), rheumatoid arthritis (RA), Sjogren's syndrome (SS), primary biliary cirrhosis (PBC), polymyositis (PM) and vasculitis has been suggested (7–12). However, the mechanism by which these B19-associated diseases affect the patient is poorly understood. Although parvovirus B19 is known to have a limited tropism in human tissues (13), B19 DNA or antigen has been found in the heart, liver, spleen, kidney, testes, skin, cerebrospinal fluid and synovium of children and adults (13, 14).

B19 is a small single-stranded DNA virus that contains 5596 nucleotides, and it has 2 large open reading frames. The genes on the left side of the genome encode the non-structural protein (NS1) and those on the right side encode 2 capsid proteins (VP1 and VP2). VP1 contains the domain that interacts with the cellular receptor; VP2 has been identified to be importantly involved in antigenic recognition by neutralizing antibodies (15, 16). The cytotoxicity of NS1 to erythroid cells has been reported and is related to the pathogenesis of B19 virus infection (17). NS1 has been reported to function as a transcription regulator by directly binding with the DNA sequence of the p6 promoter and with the Sp1/Sp3 transcription factors (18). NS1 has also been shown to be involved in DNA replication, cell cycle arrest and the initiation of apoptosis in erythroid lineage cells (19–22). Immunohistochemical analysis revealed that p53, $p21^{WAF1/CIP1}$ and caspase 3 were positive in B19-infected UT7/Epo cells (22). Additionally, NS1 has been identified to play a critical role in G1 arrest by significantly increasing the expression of $p21^{WAF1/CIP1}$; G1 arrest may be a prerequisite to apoptotic damage in cells of erythroid lineages (20, 23). However, the molecular mechanism of NS1-mediated apoptosis has not been clarified. This study identified the expression of EGFP-NS1 fusion protein in COS-7 cells, and attempted to elucidate the possible molecular mechanism of NS1-induced apoptosis in non-permissive cells.

MATERIALS AND METHODS

Plasmids and oligonucleotides

Plasmid pEGFP-C1 was obtained from CLONTECH (CLONTECH Laboratories, Palo Alto, CA, USA). This plasmid contains the EGFP variant and the neomycin resistant genes under the control of the cytomegalovirus immediate early gene promoter and the SV40 early gene promoter, respectively. Plasmid pQE40-NS1 containing non-structural (NS1) gene of human parvovirus B19 was kindly provided by Professor Susanne Modrow. The NS1 open reading frame (ORF) was obtained by PCR with primers 5′-ATGGAGCTATTTAGAGGG-3′ (forward), 5′-AAGTAGCA-

 ISSN 0036-5548

DOI: 10.1080/00365540410016230

GAAATACAGGT-3′ (reverse), which were introduced to a *Bgl* II site at the 5′ end and a *Sal* I site at the 3′ end for cloning into pEGFP-C1. The PCR was performed with reagents containing 0.2 μM primers mixtures, 1.25 μM dNTP mixture, 1.5 μM $MgCl_2$, 10 ng template, and 2.5U DNA polymerase (Takara, Tokyo, Japan). The NS1 was fused to the COOH-terminal end of EGFP (Fig. 1A). The ligatant, so-called pEGFP-NS1, was then transformed into Escherichia coli DH5α competent cells, which were obtained from Life Technologies (Carlsbad, California, USA). One set of primers was selected to amplify and confirm NS1 from constructs. Primers A is 5′-ATGGAGCTATTTAGAGGG-3′ (sense nucleotides 436–453) and primers B is 5′-AAGTAGCAGAAATACAGGT-3′ (antisense nucleotides 922–940) amplified a 505-base pair (bp) fragment corresponding to the NS1 coding sequence. Restriction enzyme digestion, PCR and DNA sequencing analysis were used to verify the plasmid.

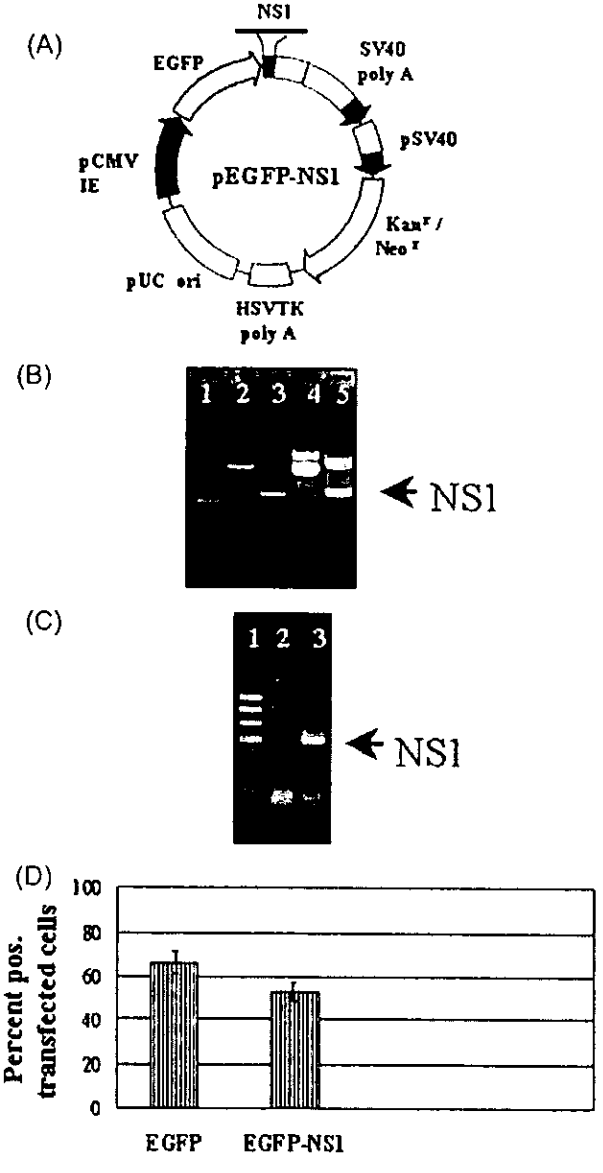

Fig. 1. Construction of pEGFP-NS1 expression vector. (A) The chematic structure of the construct pEGFP-NS1. (B) The constructs were digested with *Bgl* II and *Sal* I and separated on 1% garose gel. Lane 1 is the 1 Kb DNA ladder. Lanes 2 and 3 are EGFP and NS1 DNA, respectively. Lane 4 is the undigested EGFP-NS1. Lane 5 is the pEGFP-NS1 digested with *Bgl* II and *Sal* I. The NS1 is indicated by arrow. (C) The NS1 of the pEGFP-NS1 was reconfirmed by PCR. Lane 1 is the 1 Kb DNA ladder. Lane 2 is the mock control. Lane 3 is the PCR product of NS1 DNA. (D) The efficiency of transfect with pEGFP-C1 and pEGFP-NS1 in COS-7 cells. E = EGFP transfected cells. NS1 = NS1-transfected cells.

Cell culture and transfection

COS-7 cells were originally obtained from American type culture collection (ATCC) (Manassas, VA, USA) and were grown in Dulbecco's modified Eagle medium (DMEM) supplemented with 10% fetal bovine serum (FBS) (GIBCO-BRL, Carlsbad, California, USA) at 37°C and 5% CO_2 incubator. A total of 1×10^6 cells was grown to 70% confluent in 100 mm^2 culture plates before transfection. The transfection reaction was performed by using lipofectamine plus reagents (Invitrogene, California, USA) with 2 μg of each plasmid pEGFP-C1 or the pEGFP-NS1 constructant according to the manufacturer's instruction. The cells were then cultured in serum-free DMEM for 12 h at 37°C in a 5% CO_2 incubator and subsequently in DMEM with 10% FBS. After transfection, both pEGFP and pEGFP-NS1 transfectants were treated with neomycin (800 μg/ml), and this selection process was continued for 3 months before subsequent experiments were performed. Expressions of EGFP alone or EGFP-NS1 fusion proteins were examined by using fluorescence microscopy, Western blot analysis, flow cytometric analysis and RT-PCR.

Fluorescence microscopy

EGFP and EGFP-NS1 expression in transfected cells were observed with a Zeiss Axioplan-2 epifluorescence microscope equipped with a fluorescence filter. Digital images of the cells were recorded by using a spot camera system.

Flow cytometric analysis

The procedures for flow cytometric analysis were the same as used previously (24). The cells ($\sim 2 \times 10^6$) were fixed in 75% alcohol for 12–16 h at 4°C, followed by RNase (1 mg/ml) treatment at 25°C for 30 min. Cells were stained with propidium iodide (PI, 10 μg/ml) for 30 min before cell cycle analysis with a flow cytometer (FACScan, Becton Dickinson, Bedford, MA, USA). To detect G1-arrested cells, the cells were treated with 5 μM paclitaxel, a mitotic inhibitor (Sigma, T7402, Louis, MO, USA) for 12 h before staining with PI. For inhibition of caspase 9, cells were pretreated for 24 h with 40 μM Z-LEHD-FMK (Santa Cruz Biotechnology, Inc., Santa Cruz, California, USA) and then stained with PI.

RT-PCR

All studies were carried out in a designated PCR-clean area. RNA was extracted from infected cells using Trizol reagent (Invitrogene, Carlsbad, California, USA) according to the manufacturer's instruction. Total RNA was isolated from COS-7 cells, EGFP and EGFP-NS1 expression cells. RNA samples were resuspended in diethyl pyrocarbonate (DEPC)-treated water, quantified, and then stored at −80°C until use. RNA concentration and purity were determined by a spectrophotometer by calculating the ratio of optical density at wavelengths of 260 and 280 nm. The first-strand cDNA for RT-PCR was synthesized from total RNA (2 μg) using the Promega RT-PCR system. The cDNAs encoding human B19 NS1 and GAPDH were amplified by RT-PCR using the following primer pairs: 5′-ATGGAGCTATTTAGAGGG-3′ (forward primer for NS1 cDNAs), 5′-AAGTAGCAGAAATACAGGT-3′ (reverse primer for NS1 cDNAs), 5′-CATGTTCGTCATGGGTGTGA-3′ (forward primer for GAPDH cDNAs), and 5′-AGTGAGCTT

CCCGTTCAGCTC-3′ (reverse primer for GAPDH cDNAs). The amplification was performed in a 50 µl reaction volume containing 1× reaction buffer (Promega, Madison, Wisconsin, USA), 1.5 µM of $MgCl_2$, 200 µM of dNTPs, 1 µM of each primer and 2.5 units of Taq DNA polymerase (Promega, Madison, Wisconsin, USA) using a Perkin-Elmer Gene Amp PCR system 2400. Each cycle consists of denaturation at 95°C for 1 min, annealing at 55°C for 45 s, and amplification at 72°C for 45 s. The RT-PCR derived DNA fragments obtained by 30 PCR cycles were subjected to electrophoresis on a 1.7% agarose gel.

DNA fragmentation analysis

DNAs from COS-7 cells, EGFP, and EGFP-NS1 transfectants were solated in lysis buffer (20 mM Tris, 10 mM EDTA, 0.2% Triton X-100) at 4°C for 10 min. After centrifugation at 12,000 rpm for 5 min, he supernatant was transferred to new tubes and supplemented with 12.5 µl of proteinase K (25 mg/ml) at 50°C for 6 h, followed by extraction in phenol, chloroform, and a final ethanol precipitation vas performed. After RNase digestion at 10 mg/ml for 1 h at 37°C, dentical amounts of DNA were separated on 1.5% agarose gel by electrophoresis at 25°C.

Caspase 3 activity assay

A caspase 3 ELISA kit (BD Pharmingen, San Diego, California, USA) was used for in vitro determination of caspase 3 enzymatic activity in cell lysates as instructed by the manufacturer.

SDS-PAGE and Western blotting

Cells were lysed in an aliquot volume of whole-cell extraction buffer A (140 mM NaCl, 10 mM Tris, pH 7.5, 1.5 mM $MgCl_2$, 0.5% NP-40) and protease inhibitor cocktail (Roche Diagnostics GmbH, Roche Applied Science, Mannheim, Germany) for 30 min on ice. Cell lysates were then microcentrifuged at 14,000 rpm for 10 min to remove the insoluble component. 30 µg of protein from the supernatants was separated by 12.5% sodium dodecyl sulfate-polyacrylamide gel electrophoresis (SDS-PAGE). Samples were applied to the gel and separated at 100–150 V for 1.5 h. The gel was then electrophoretically transferred to nitrocellulose, according to the method of Towbin et al. (25). The strips were washed twice with PBS-Tween for 1 h and incubated with secondary antibody consisting of alkaline phosphatase conjugated goat anti-rabbit or mouse IgG antibodies. The substrate of nitroblue tetrazolium/5-bromo-4-chloro-3 indolyl phosphate (NBT/BCIP) was used to detect the reaction. For inhibition of p53, the cells were pretreated for 12 h with 10 µM p53 inhibitor (Pifithrih-a hydrobromide) (26) and then processed as described vide supra. Mouse anti-actin monoclonal antibody was purchased from Cashmere Biotech (Houston, Texas, USA). Anti-caspase 3 antibody, anti-$p21^{WAF1/CIP1}$ monoclonal antibody, anti-p53 monoclonal antibody, and anti-human $p16^{INK4}$ monoclonal antibody were purchased from Pharmingen International. Anti-B19 NS1 antibody was made by immunization of recombinant His-tag NS1. Anti-GFP antibody was purchased from Invitrogen. Anti-caspase 8 antibody, anti-caspase 9 antibody, and caspase 9 inhibitor (Z-LEHD-FMK) were purchased from Santa Cruz Biotechnology, Inc (Santa Cruz, CA, USA). The p53 inhibitor (Pifithrih-a hydrobromide) was purchased from Tocris Cookson Inc. Ellisville, MO, USA).

Statistical analysis

The paired *t*-test was used to analyze for statistical significance. A *p*-value <0.05 was considered significant.

RESULTS

Construction of human parvovirus B19 non-structural protein NS1 in pEGFP-C1 vector

The construction of the NS1 gene into the COOH terminus of EGFP vector as pEGFP-NS1 is shown in Fig. 1A. The constructs were digested by restriction enzymes *Bgl* II and *Sal* I separated by 1% agarose gel (Fig. 1B). Lane 1 is the 1 Kb DNA ladder. Lanes 2 and 3 are pEGFP and NS1 DNA. Lane 4 is the undigested construct of pEGFP-NS1. Lane 5 is the pEGFP-NS1 digested with *Bgl* II and *Sal* I, and there is a 2029 bp fragment of NS1. The NS1 is indicated by an arrow. The NS1 DNA of the construct was reconfirmed by PCR (Fig. 1C) and by sequencing before transfection.

Expression of EGFP and EGFP-NS1 in COS-7 cells

Both pEGFP-C1 and pEGFP-NS1 vectors were successfully transfected into COS-7 cells as transfectants EGFP and EGFP-NS1, respectively. We achieved 50–70% transfection efficiency (Fig. 1D). COS-7 cells expression EGFP-NS1 fusion proteins revealed specific cytoplasmic staining by immunofluorescence, while the cells expression EGFP only revealed both nuclear and cytoplasmic staining by immunofluorescence (Fig. 2A). The localization of EGFP-NS1 fusion proteins was consistent with the previous report by indirect immunofluorescence (27). The EGFP fluorescence (blank peak) was observed in both transfectants by fluorescence microscopy. The visualization of fluorescence indicated that both EGFP and NS1 vectors had been transfected into the COS-7 cells (Fig. 2B). The dark peak represents the COS-7 cells as the background by flow cytometry analysis (Fig. 2B). The expression of NS1 mRNA and NS1 protein in the NS1 transfected cell was also confirmed by RT-PCR (Fig. 2C) and Western blot (Fig. 2D). The EGFP-NS1 fusion protein was migrating at the predicted molecular weight of 104 kDa with rabbit anti-NS-1 antibody on immunoblot (Fig. 2D).

NS1 expression delays cell cycle progression at G1 phase and activates the expression of p53, $p21^{WAF1/CIP1}$, and p16 in NS1-transfected cells

It is known that NS-1 protein can induce G1 cell cycle arrest and apoptosis in erythroid lineage such as K562 and UT7/EpO-S1 cell lines (20–22, 28). To verify the role of NS1 protein in COS-7 cells, COS-7, EGFP and EGFP-NS1 cell lines were treated with paclitaxel for 12 h and analyzed by flow cytometry. The cells at G0/G1 phase of COS-7 and EGFP cell lines treated with paclitaxel were 11.7% and 8.9%, respectively. However the cells at the G0/G1 phase of EGFP-NS1 cell line treated with paclitaxel were 34.1% (Fig. 3A, lower panel). These results indicate that NS1 expression delays the cell cycle progression at the G1 phase. In these NS1-transfected cells the expression of p53, an important molecule in cell cycle regulation, and its downstream cell cycle kinase inhibitors $p21^{WAF1/CIP1}$ and $p16^{INK4}$

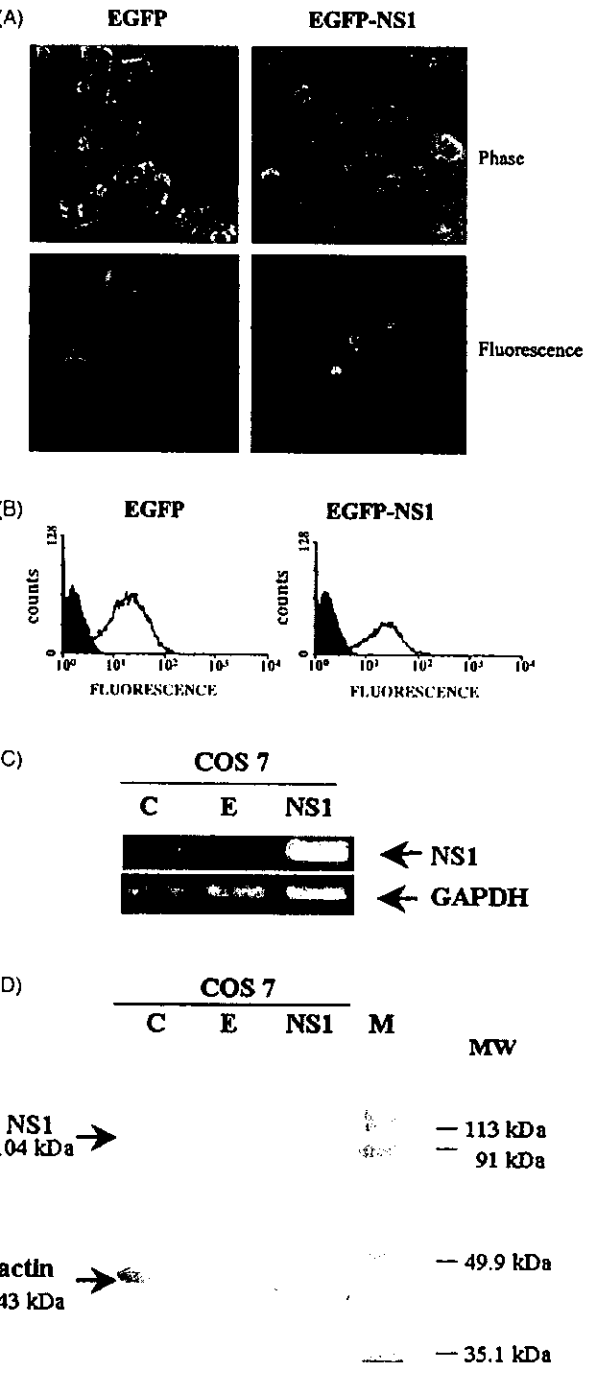

ig. 2. Expression of EGFP alone and EGFP-NS1 fusion protein in OS-7 cells. (A) Visualization of EGFP (left panel) and EGFP-NS1 ight panel) by fluorescence microscopy. The NS1-transfected cells ow specific cytoplasmic fluorescence staining. (B) Analysis of the xpression of EGFP and EGFP-NS1 fusion protein with fluores-nce by flow cytometry. The dark peak represents the non-ansfected COS-7 cells as the background. The blank peak was om both transfected EGFP and EGFP-NS1 cells. (C) RT-PCR nd (D) Western blot analysis of the expressed fusion proteins. I = molecular weight standards. C = COS-7 cells. E = EGFP trans-cted cells. NS1 = NS1-transfected cells. GAPDH and actin were ie controls. MW = molecular weight. The EGFP-NS1 fusion rotein is indicated by arrow.

were analyzed by Western blot. The expressions of p53, $p21^{WAF1/CIP1}$, and $p16^{InK4}$ were increased (Fig. 3B). The results indicates that NS1 expression may delay the G1 cell cycle progression and it may contribute to the p53/$p21^{WAF1/CIP1}$-dependent pathway, which is consistent with the previous report (12).

NS1 expression induces apoptosis in COS-7 cells

The NS1-transfected cells were analyzed for apoptosis by flow cytometry, ELISA and DNA gel electrophoresis. The sub-G1 phase in the NS1-transfected cells was significantly higher than that in both EGFP cells and COS-7 cells (Fig. 4A). The cells at sub-G1 phase of COS-7, EGFP and EGFP-NS1 transfected cells were 0.1%, 8% and 18%, respectively. The cells at sub-G1 phase indicated that cells were undergoing apoptosis. It is not surprising that apoptosis occurred in EGFP-transfected COS-7 cells in the present study. To ascertain if the caspases participate in NS1-induced apoptosis, a critical downstream protease caspase 3 was evaluated in the transfected cells. Substantial caspase 3 activity was induced by NS1 expression in the cells by ELISA. The difference was statistically significant between EGFP and EGFP-NS1 transfection in COS-7 cells ($p = 0.0002$) (Fig. 4B). Genomic DNA extracted from NS1-transfected cells and EGFP cells also revealed the presence of DNA fragments, and the typical characteristic of apoptosis (Fig. 4C). These results showed that apoptosis could be induced by the expression of NS1 in NS1-transfected cells. NS1-induced apoptosis was demonstrated by the appearance of sub-G1 phase, increased caspase 3 activity, and DNA fragmentation in the NS1-transfected cells.

NS1-induced apoptosis occurs through the mitochondrial cell death pathway

To further investigate the mechanism of NS1-induced apoptosis, a number of apoptosis-associated proteins were analyzed with specific antibodies by Western blot. The induction of Bax and Bad proteins was detected (Fig. 5A), which were known as the mitochondrial-associated pro-apoptotic proteins (29, 30). The activation of caspase 3 and caspase 9 (Fig. 5A), but not the activation of caspase 8 (Fig. 5B) or Fas (Fig. 5A) was detected in the NS1-transfected cells. Furthermore, the NS1-transfected cells were treated with the p53 inhibitor, Pifithrih-α hydrobromide, and the caspase 9 inhibitor, Z-LEHD-FMK. The sub-G1 phase was analyzed by flow cytometry before and after the caspase 9 inhibitor treatment in COS-7, EGFP and EGFP-NS1 cells. The cells at sub-G1 phase of NS1-transfected cells before and after Z-LEHD-FMK treatment were 15% and 2%. The sub-G1 phase was eliminated after Z-LEHD-FMK treatment for 24 h in the NS1-transfected cells (Fig. 6A, lower, right panel). The expression of caspase 9, p53, Bax, and p21 were markedly eliminated by the p53 inhibitor, Pifithrih-α hydrobromide (Fig. 6B, right panel). The apoptosis of

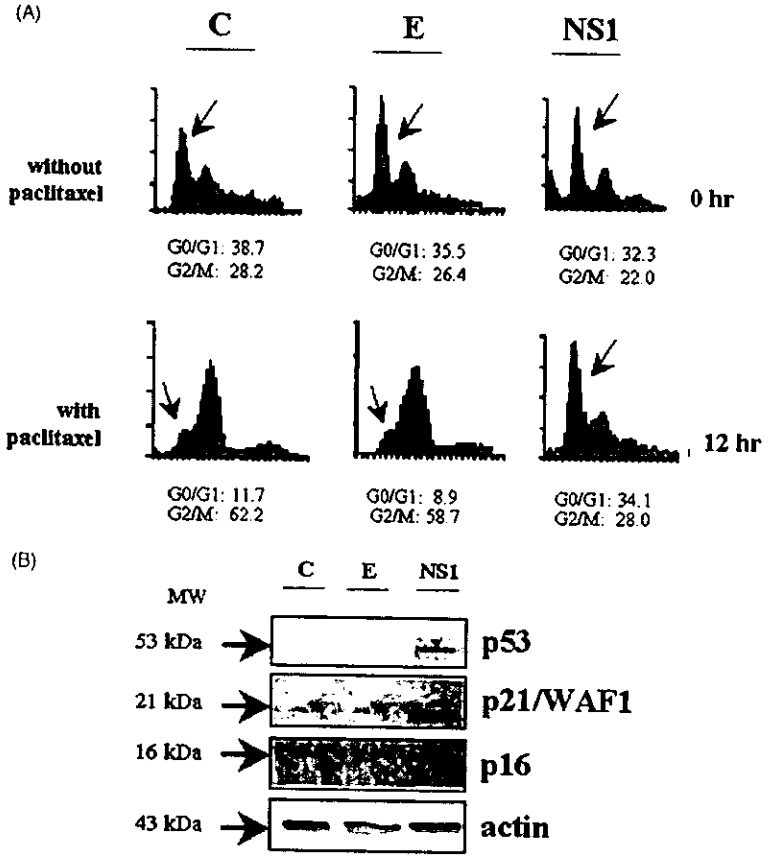

ig. 3. NS1 expression delays cell cycle progression at G1 phase and activates the expression of p53, p21, and p16 in NS1-transfected cells. A) COS-7, EGFP, and EGFP-NS1 expression clones were treated with paclitaxel (5 μM) for synchronization at G2 phase and analyzed by ow cytometry. Arrows indicate G1 phase cells. The percentages of G0/G1and G2/M cells were calculated and shown in the diagrams. The pression of NS1 delayed the cell cycle progression at G1 phase in the NS1-transfected cells. (B) Expression of p53, p21, and p16 was creased in the NS1-transfected cells by Western blot. C = COS-7 cells. E = EGFP transfected cells. NS1 = NS1-transfected cells. Actin is the ntrol. MW = molecular weight.

S1-transfected cells was inhibited by both the caspase 9 nd the p53 inhibitors. From these results, it is strongly ggested that p53 is involved in the EGFP- and EGFP-NS1 duced apoptosis in COS-7 cells. These results showed that 53-induced Bax expression and subsequent activation of spase 9 was probably the major apoptotic pathway in S1-induced apoptosis and suggests that NS1-induced optosis in COS-7 cells occurs through the mitochondria-ediated apoptosis pathway (31, 32).

ISCUSSION

uman parvovirus B19 has been found in various tissues -8, 33, 34), suggesting that extensive B19-infectious rgets may exist. This finding inspired us to investigate e possible role of NS1 in B19 non-permissive cells. COS-7 lls are known to be potentially useful for identifying B19 al structural and non-structural proteins (35).

The expression of EGFP-NS1 in COS-7 cells was identi-d (Figs. 1 and 2) to understand better the pathogenesis of 9 in non-permissive target cells. The progression of the cell cycle was delayed in the G1 phase in the presence of NS1 protein, and apoptosis was induced subsequently (Figs. 3 and 4). Furthermore, mitochondria-related apoptotic proteins were observed (Fig. 5) and the induction of caspase 9 was suppressed by both p53 and caspase 9 inhibitors (Z-LEHD-FMK); the caspase 9 inhibitor significantly reduced NS1-induced apoptosis (Fig. 6).

Previous studies have shown that NS1 expression induces apoptosis in erythroid linage cells (12, 21, 22, 28, 36), but the mechanism in non-permissive cells remains unclear. Moffatt et al. (28) first reported the NS1-induced apoptosis in human erythroid cell lines, and the apoptosis was mitigated by the caspase 3 inhibitor and Bcl-2 overexpression. The authors inferred that NS1 induces cell death by activating caspase 3. Sol et al. (21) found that caspase 3, 6, and 8 inhibitors inhibited NS1-induced apoptosis. The activation of caspase 3, 6, and 8 was induced by NS1 expression. The authors suggested that NS1 might interact with tumor necrosis factor alpha (TNF-α) in the apoptotic pathway. In contrast, the present study found increased expression of the pro-apoptotic Bcl-2 members Bax and Bad, and the activation of

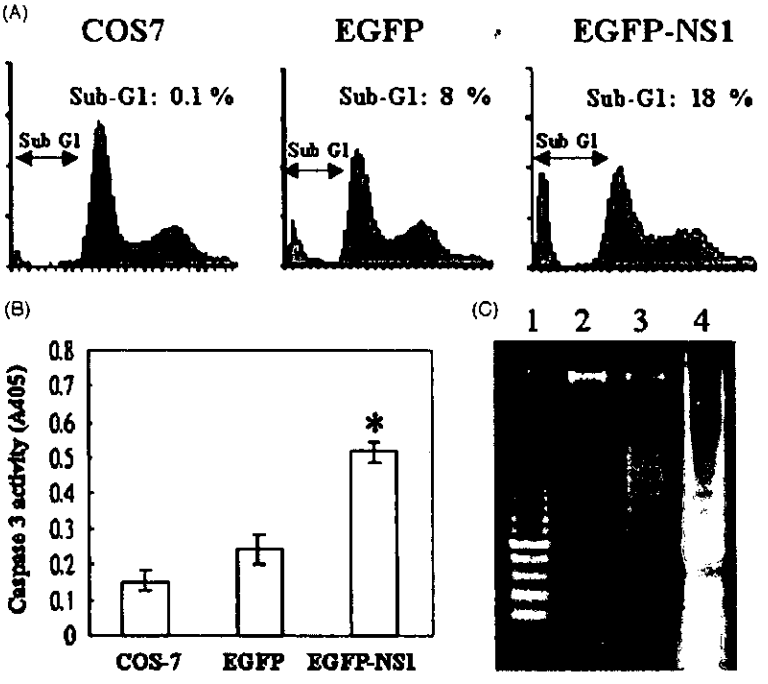

Fig. 4. Expression of NS1 induces cell death. The sub-G1 phase in the NS1-transfected cells was significantly higher than that in the both EGFP cells and COS-7 cells by flow cytometry analysis (Fig. 4A). The sub-G1 phase represents apoptotic cells. The activities of caspase 3 were increased in EGFP-NS1 transfected cells by ELISA. * Statistically significant difference (Fig. 4B). The DNA fragments were detected by DNA gel electrophoresis (Fig. 4C). Lane 1 is the 100 bp DNA ladder. Lanes 2, 3 and 4 are genomic DNA extracted from COS-7 cells, and EGFP and NS1 transfected cells, respectively.

caspase 3 and caspase 9, but not of caspase 8 or Fas, in NS1-transfected cells. We propose that apoptosis is initiated by the pathway of emergence from mitochondria by activating p53 and Bax, and by the subsequent activation of caspase 9, since apoptosis was significantly inhibited by the caspase 9 and p53 inhibitors.

The data presented here imply that the up-regulation of $p21^{WAF1/CIP1}$ as a result of the presence of NS1, delays the cell cycle at the G1 stage in COS-7 cells. This finding is consistent with results published elsewhere, that NS1 expression induced arrest of UT7/EPO-S1 cells in the G1 stage by the induction of $p21^{WAF1/CIP1}$ (20). Moreover, NS1-transfected cells exhibited increased p53 expression (Fig. 6), indicating the involvement of a p53-dependent pathway for $p21^{WAF1/CIP1}$ -induced G1 arrest. Thus, the activity of NS1-induced p53 is under investigation. In this study, the apoptosis was observed by FACS analysis and the related apoptotic proteins were examined by Western blot; they were thus identified as mitochondria-related apoptotic proteins. This is the first report to state that NS1-induced apoptosis in B19 non-permissive cells may follow the pathway of mitochondria cell death. The data reveal that G1 arrest is associated with NS1, suggesting that subsequent apoptosis may be mediated by NS1 through the induction of G1 arrest and caspase activation.

The role of the viral cytopathic effect in the pathogenesis of B19-associated organ involvement remains unclear. The elucidation here of the NS1-induced apoptosis pathway

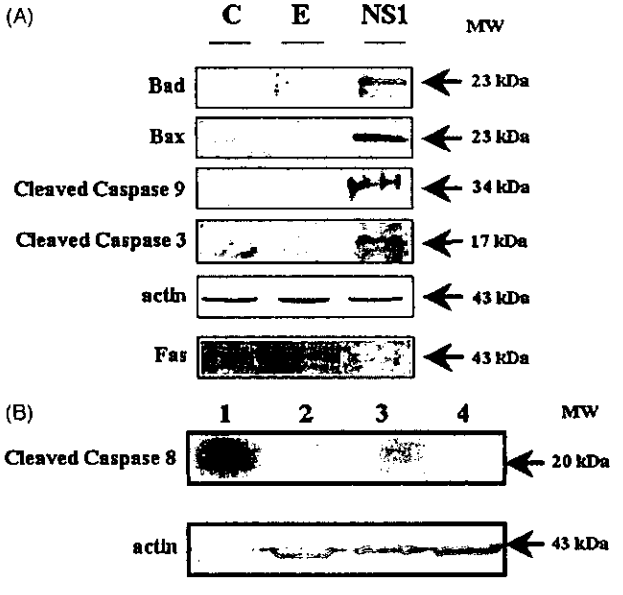

Fig. 5. Apoptosis-associated proteins were analyzed by Western blot. Increased expressions of the pro-apoptotic Bcl-2 members Bax, Bad and the activation of caspase 3 and caspase 9 (Fig. 5A), but not the activation of caspase 8 (Fig. 5B) and Fas (Fig. 5A) were detected in the NS1-transfected cells. In Fig. 5B, Lane 1 is lysate from H460 cells treated with TRAIL (100 ng/ml) for 12 h as a positive control. Lanes 2, 3 and 4 are lysates from COS-7 cells, and EGFP and NS1-transfected cells, respectively. Actin is the control. MW =molecular weight.

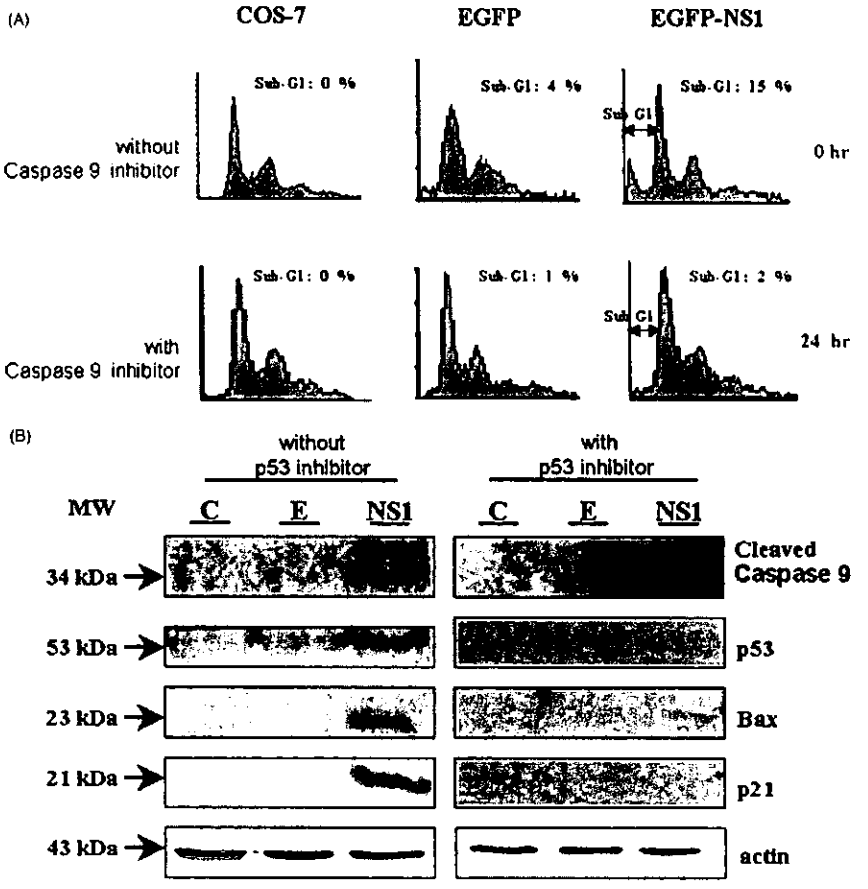

Fig. 6. NS1-induced apoptosis was inhibited by both the caspase 9 inhibitor, Z-LEHD-FMK and the p53 inhibitor, Pifithrih-α hydrobromide. (A) The sub-G1 phase was analyzed by flow cytometry before (upper panel) and after (lower panel) caspase 9 inhibitor treatment in COS-7, EGFP and EGFP-NS1 cells. Apoptosis was completely inhibited by the caspase 9 inhibitor in the EGFP-NS1 cells (lower, right panel). (B) The expressions of caspase 9, Bax, p21, and p53 were analyzed with Western blot after treatment with the p53 inhibitor (right panel). The expressions of cleaved caspase 9, p53, Bax, and p21 were abolished by the p53 inhibitor treatment. Actin is the control. MW = molecular weight.

through mitochondria may provide further information on the pathogenesis of diseases with associated parvovirus-B19.

ACKNOWLEDGEMENTS

We thank Professor Susanne Modrow, Institute for Medical Microbiology, Universität Regensburg, Regensburg, Germany for the generous gift of the pQE40-NS1 plasmid. This study was supported by the grants NSC 90-2314-B040-009 and NSC 91-2314-B040-005 from the National Science Council, Taiwan, and CSMU 88-CM-B-038 from Chung Shan Medical University, Taiwan.

REFERENCES

1. Cossart YE, Field AM, Cant B, Widdows D. Parvovirus-like particles in human sera. Lancet 1975; 1: 72–3.
2. Finkel TH, Torok TJ, Ferguson PJ, Durigon EL, Zaki SR, Leung DY, et al. Chronic parvovirus B19 infection and systemic necrotizing vasculitis: opportunistic infection or etiological agent? Lancet 1994; 343: 1255–8.
3. Nesher G, Osborn TG, Moore TL. Parvovirus infection mimicking systemic lupus erythematosus. Semin Arthritis Rheum 1995; 24: 297–303.
4. Bultmann BD, Klingel K, Sotlar K, Bock CT, Kandolf R. Parvovirus B19: a pathogen responsible for more than hematologic disorders. Virchows Arch 2003; 442: 8–17.
5. Chou CTN, Hsu TC, Chen RM, Lin LI, Tsay GJ. Parvovirus B19 infection associated with the production of anti-neutrophil cytoplasmic antibody (ANCA) and anticardiolipin antibody (aCL). Lupus 2000; 9: 551–4.
6. Von Landenberg P, Lehmann HW, Knoll A, Dorsch S, Modrow S. Antiphospholipid antibodies in pediatric and adult patients with rheumatic disease are associated with parvovirus B19 infection. Arthritis Rheum 2003; 48: 1939–47.
7. Hsu TC, Tsay GJ. Human parvovirus B19 infection in patients with systemic lupus erythematosus. Rheumatology (Oxford) 2001; 40: 152–7.
8. Kalish RA, Knopf AN, William Gary G, Canoso JJ. Lupus-like presentation of human parvovirus B19 infection. J Rheum 1992; 19: 169–71.
9. Takahashi Y, Murai C, Shibata S, Munakata Y, Ishii T, Ishii K, et al. Human parvovirus B19 as a causative agent for rheumatoid arthritis. Proc Natl Acad Sci USA 1998; 95: 8227–32.
10. Trapani S, Ermini M, Falcini F. Human parvovirus B19 infection: its relationship with systemic lupus erythematosus. Semin Arthritis Rheum 1999; 28: 319–25.

1. Lehmann HW, von Landenberg P, Modrow S. Parvovirus B19 infection and autoimmune disease. Autoimmun Rev 2003; 2: 218–23.
2. Morita E, Sugamura K. Human parvovirus B19-induced cell cycle arrest and apoptosis. Springer Semin Immunopathol 2002; 24: 187–99.
3. Soderlund-Venermo M, Hokynar K, Nieminen J, Rautakorpi H, Hedman K. Persistence of human parvovirus B19 in human tissues. Pathol Biol (Paris) 2002; 50: 307–16.
4. Hokynar K, Soderlund-Venermo M, Pesonen M, Ranki A, Kiviluoto O, Partio EK, Hedman K. A new parvovirus genotype persistent in human skin. Virology 2002; 302: 224–8.
5. Pattison JR. Human parvoviruses. In: Zuckerman AJ, Banatvala JE, Pattison JR, eds. Principles and practice of clinical virology. New York: John Wiley and Sons, Ltd; 2000. p. 645–58.
6. Young NS. Parvoviruses. In: Fields BN, Knipe DM, Howley PM, et al, eds. Fields virology. Philadelphia: Lippincott Raven; 1996. p. 2199–236.
7. Ozawa K, Ayub J, Kajigaya S, Shimada T, Young N. The gene encoding the non-structural protein of B19 (human) parvovirus may be lethal in transfected cells. J Virol 1988; 62: 2884–9.
8. Raab U, Beckenlehner K, Lowin T, Niller HH, Doyle S, Modrow S. NS1 protein of parvovirus B19 interacts directly with DNA sequences of the p6 promoter and with the cellular transcription factors Sp1/Sp3. Virology 2002; 293: 86–93.
9. Koch WC. Fifth (human parvovirus) and sixth (herpes virus 6) disease. Curr Opin Infect Dis 2001; 14: 343–56.
10. Morita E, Nakashima A, Asao H, Sato H, Sugamura K. Human parvovirus B19 nonstructuralprotein (NS1) induces cell cycle arrest at G(1) phase. J Virol 2003; 77: 2915–21.
11. Sol N, Le Junter J, Vassias I, Freyssinier JM, Thomas A, Prigent AF, et al. Possible interactions between the NS1 protein and tumor necrosis factor alpha pathways in erythroid cell apoptosis induced by human parvovirus B19. J Virol 1999; 73: 8762–70.
12. Yaegashi N, Niinuma T, Chisaka H, Uehara S, Moffatt S, Tada K, et al. Parvovirus B19 infection induces apoptosis of erythroid cells in vitro and in vivo. J Infect 1999; 39: 68–76.
13. Gartel AL, Tyner AL. The role of the cyclin-dependent kinase inhibitor p21 in apoptosis. Mol Cancer Ther 2002; 1: 639–49.
14. Tzang BS, Chiang YJ, Lan HC, Liao CB, Liu YC. Tuning up or down the UV-induced apoptosis in Chinese hamster ovary cells with cell cycle inhibitors. Photochem Photobiol 2002; 75: 662–7.
25. Towbin H, Staehelin T, Gordon J. Electrophoretic transfer of proteins from polyacrylamide gels to nitrocellulose sheets: procedure and some applications. Proc Natl Acad Sci USA 1979; 76: 4350–4.
26. Komarov PG, Komarova EA, Kondratov RV, Christov-Tselkov K, Coon JS, Chernov MV, Gudkov AV. A chemical inhibitor of p53 that protects mice from the side-effects of cancer therapy. Science 1999; 285: 1733–7.
27. St Amand J, Astell CR. Identification and characterization of a family of 11-kDa proteins encoded by the human parvovirus B19. Virology 1993; 192: 121–31.
28. Moffatt S, Yaegashi N, Tada K, Tanaka N, Sugamura K. Human parvovirus B19 non-structural (NS1) protein induces apoptosis in erythroid lineage cells. J Virol 1998; 72: 3018–28.
29. Degli Esposti M, Dive C. Mitochondrial membrane permeabilization by Bax/Bak. Biochem Biophys Res Commun 2003; 304: 455–61.
30. Falke D, Fisher M, Ye D, Juliano RL. Design of artificial transcription factors to selectively regulate the pro-apoptotic bax gene. Nucleic Acids Res 2003; 31: e10.
31. Marchenko ND, Zaika A, Moll UM. Death signal-induced localization of p53 protein to mitochondria: a potential role in apoptotic signaling. J Biol Chem 2000; 275: 16202–12.
32. van Gurp M, Festjens N, van Loo G, Saelens X, Vandenabeele P. Mitochondrial intermembrane proteins in cell death. Biochem Biophys Res Commun 2003; 304: 487–97.
33. Schwarz TF, Wiersbitzky S, Pambor M. Case report: detection of parvovirus B19 in a skin biopsy of a patient with erythema infectiosum. J Med Virol 1994; 43: 171–4.
34. Takahashi M, Ito M, Sakamoto F, Shimizu N, Furukawa T, Takahashi M, Matsunaga Y. Human parvovirus B19 infection: immunohistochemical and electron microscopic studies of skin lesions. J Cutan Pathol 1995; 22: 168–72.
35. Cohen BJ, Field AM, Mori J, Brown KE, Clewley JP, St Amand J, Astell CR. Morphology and antigenicity of recombinant B19 parvovirus capsids expressed in transfected COS-7 cells. J Gen Virol 1995; 76: 1233–7.
36. Chisaka H, Morita E, Murata K, Ishii N, Yaegashi N, Okamura K, Sugamura K. A transgenic mouse model for non-immune hydrops fetalis induced by the NS1 gene of human parvovirus B19. J Gen Virol 2002; 83: 273–81.

Submitted February 16, 2004; accepted May 17, 2004

拾、九十三年度計畫執行情形

註：群體計畫(PPG)者，不論是否提出各子計畫資料，都必須提出總計畫整合之資料
若為群體計畫，請勾選本表屬於：□子計畫； 或 □總計畫(請自行整合)

一、 請簡述原計畫書中，九十三年預計達成之研究內容

九十三年預計達成之研究內容為：

一、探討急性酒精暴露對老鼠腹腔巨噬細胞數目及其免疫功能的影響

1. 急性酒精暴露對老鼠腹腔巨噬細胞數目的影響
2. 急性酒精暴露對老鼠腹腔巨噬細胞吞噬能力的影響
3. 急性酒精暴露對老鼠腹腔巨噬細胞釋放一氧化氮能力的影響
4. 急性酒精暴露對老鼠腹腔巨噬細胞釋放過氧化氫能力的影響
5. 急性酒精暴露對老鼠腹腔巨噬細胞釋放腫瘤壞死因子能力的影響
6. 急性酒精暴露對老鼠腹腔巨噬細胞釋放細胞激素(IL-12)能力的影響
7. 急性酒精暴露對老鼠腹腔巨噬細胞毒殺腫瘤細胞能力的影響

二、探討內分泌物質及細胞激素在急性酒精暴露下對老鼠腹腔巨噬細胞數目及其免疫功能方面所扮演的角色

1. 糖皮質素(glucocorticoids)在急性酒精暴露下對老鼠腹腔巨噬細胞數目及其免疫功能方面所扮演的角色
2. 兒茶酚胺(catecholamines)在急性酒精暴露下對老鼠腹腔巨噬細胞數目及其免疫功能方面所扮演的角色

二、 請詳述九十三年度計畫執行情形，並評估是否已達到原預期目標（請註明達成率）

本篇研究以 B6C3F1 母鼠為實驗動物，32 %（6.0 g/kg）的酒精劑量為實驗劑量，探討在急性酒精暴露下，對腹腔內巨噬細胞的細胞數目及其免疫功能，包括吞噬作用、釋放過氧化氫、一氧化氮及腫瘤壞死因子能力和毒殺腫瘤細胞能力的影響。研究結果發現酒精會減少腹腔巨噬細胞的細胞數目及抑制上述所列之免疫功能。另外加入 thioglycollate 模擬生物體受到

細菌感染時的情形，也發現酒精會降低腹腔巨噬細胞數及其免疫功能。我們也使用 RU486（糖皮質素受器的拮抗劑）探討糖皮質素(glucocorticoids)對急性酒精降低腹腔巨噬細胞的細胞數目及抑制免疫功能所扮演的角色，結果顯示酒精誘導生成的糖皮質素的確會降低巨噬細胞的細胞數目及其免疫功能。除了酒精對腹腔巨噬細胞釋放細胞激素(IL-12)能力的影響外，本計畫目前的執行結果已大部分達到原預期目標。目標達成率約為 90%。